Sustainable Valorization of Olive Pomace into Biochar–Pectin Composite for Enhanced Water Retention and Plant Growth in Arid Agriculture

Raid Alrowais,[a,]* Mahmoud M. Abdel-Daiem,[b,]* Rania Saber Yousef,[c]
Osama Konsowa Ahmed,[c] and Noha Said [b]

* Corresponding authors: rnalrowais@ju.edu.sa; mmabdeldaiem@eng.zu.edu.eg

DOI: 10.15376/biores.21.4.10921-10957

GRAPHICAL ABSTRACT

Sustainable Valorization of Olive Pomace into Biochar–Pectin Composite for Enhanced Water Retention and Plant Growth in Arid Agriculture

Raid Alrowais,[a,]* Mahmoud M. Abdel-Daiem,[b,]* Rania Saber Yousef,[c]
Osama Konsowa Ahmed,[c] and Noha Said [b]

Agro-industrial residues from the olive oil industry present considerable environmental challenges due to their high organic load and phytotoxic phenolic content. This study explored the valorization of olive pomace by developing pectin, pectin gel, and a biochar–pectin gel composite (BPGC) for sustainable agricultural applications. The materials were characterized using Fourier transform infrared spectroscopy, scanning electron microscopy, and Brunauer–Emmett–Teller analysis, confirming successful composite formation and revealing the predominantly mesoporous characteristics of the olive pomace-derived biochar. Swelling analysis showed that pectin reached 121% within 10 min and 195% after 2 h, while BPGC exhibited superior moisture retention (60%) and water-holding capacity (97.9%). Germination studies demonstrated high seed viability (96% to 98%) across treatments, with BPGC producing the highest seedling-growth responses, including shoot length of 8.31 cm, root length of 4.03 cm, and a seedling vigor index of 1210. Enzymatic activity was also improved, with protease and lipase reaching 186 and 201 U/g FW, respectively, in BPGC-treated samples. No detectable phytotoxic effects were observed under the tested conditions. These findings indicate that BPGC is a promising bio-based water-retaining soil amendment for improving soil moisture management and early plant growth, particularly in arid and semi-arid agricultural systems.

DOI: 10.15376/biores.21.4.10921-10957

Keywords: Olive pomace valorization; Pectin hydrogel; Water retention; Sustainable agriculture; Circular economy; SDG 6: Clean water and sanitation; SDG 9: Industry, Innovation and Infrastructure

Contact information: a: Department of Civil Engineering, College of Engineering, Jouf University, Sakakah 72388, Saudi Arabia; b: Environmental Engineering Department, Faculty of Engineering, Zagazig University, Zagazig, 44519, Egypt; c: Biochemistry Department, Faculty of Agriculture, Cairo University, Giza, 12613, Egypt;
** Corresponding authors: rnalrowais@ju.edu.sa; mmabdeldaiem@eng.zu.edu.eg*

INTRODUCTION

Water scarcity is regarded as one of the major global challenges, particularly in arid and semi-arid regions such as the Mediterranean, North Africa, and the Middle East (Sun *et al.* 2025). Water-retaining soil amendments and irrigation-management technologies represent complementary strategies for improving agricultural water-use efficiency under drought conditions (FAO 2021). Recent studies indicate that incorporating superabsorbent polymers into soil can reduce irrigation requirements by 15 to 50% while maintaining crop growth under water-stress conditions (Abdelfattah and Mostafa 2024).

Recent advances in precision agriculture have highlighted the potential of Internet of Things (IoT)-based irrigation systems to improve water-use efficiency through real-time soil-moisture sensing, environmental monitoring, and automated irrigation control (Pérez *et al*. 2024). Correa-Quiroz *et al.* (2025), for example, demonstrated an ESP32-based system for greenhouse monitoring and automated drip irrigation. Bio-based water-retaining soil amendments could complement such technologies by conserving moisture within the root zone, providing an integrated material–digital strategy for climate-resilient agriculture in arid and water-scarce regions.

The olive oil industry generates substantial quantities of solid and liquid waste that pose significant environmental risks if improperly managed. Mediterranean countries, including Spain, Italy, Greece, Tunisia, Morocco, and Egypt, as well as Saudi Arabia generate large quantities of olive pomace annually, a solid residue generated during olive oil extraction (Sun *et al.* 2025). Olive pomace is characterized by high organic matter and lignocellulosic contents and contains phenolic compounds that may contribute to phytotoxic effects when inadequately managed (Raihani *et al.* 2025).

Traditional disposal methods, such as burning agricultural waste or uncontrolled dumping, cause air and groundwater pollution (Gómez-Cruz *et al.* 2024). Nevertheless, olive pomace is also a valuable source of bioactive and functional components, including polyphenols, oleuropein, hydroxytyrosol, pectin, and lignocellulosic fractions that can potentially be recovered or converted into value-added products. Despite this valuable composition, olive by-products remain largely underutilized for high-value applications, highlighting the need for sustainable valorization strategies that convert these residues into functional materials within a circular-bioeconomy framework (Sun *et al.* 2025).

Among the valuable components of olive pomace, pectin is a structural heteropolysaccharide of plant cell walls that can be recovered through acid-assisted aqueous extraction (Kanagalakshmi *et al.* 2024). Pectin is structured from α-D-galacturonic acid units linked by α-(1 → 4) glycosidic bonds, with variable degrees of methylation. Pectin possesses several properties relevant to agricultural applications, including high hydrophilicity, water-retention capacity, biodegradability, and the ability to form crosslinked polymer networks (Rubio-Martin del Campo *et al.* 2025). In particular, low-methoxyl pectin can form three-dimensional hydrogel networks through ionic crosslinking with divalent cations such as Ca^{2+}, enabling substantial water uptake and retention (Gawkowska *et al.* 2018).

Within biochar–pectin composites, pectin can potentially perform a dual function. Before gelation, its carboxylate groups ($–COO^-$) may facilitate dispersion and stabilization of biochar particles within the aqueous polymer phase. Following Ca^{2+}-induced gelation, the interconnected pectin network acts as a structural binder that physically immobilizes the biochar particles within the composite (Wang *et al.* 2021; Said *et al.* 2023; Rubio-Martin del Campo *et al.* 2025).

Pectin hydrogels are of great interest because of their biocompatibility, biodegradability, and non-toxicity (Rubio-Martin del Campo *et al.* 2025). Recent studies have demonstrated the potential of pectin-based hydrogels for agricultural applications, including soil erosion control and water conservation, by functioning as water reservoirs that retain moisture and gradually release it within the plant root zone during water-deficit periods (Kanagalakshmi *et al.* 2024; Morán-Alarcón *et al.* 2026).

Converting agricultural residues into functional biochar represents an important strategy for advancing circular-bioeconomy approaches and developing sustainable soil amendments. The physicochemical properties, pore architecture, and surface functionality of biomass-derived biochar are strongly influenced by feedstock composition, chemical treatment, and thermal conversion conditions (Hou *et al.* 2022; Wijitkosum and Sriburi 2025; Chafi *et al.* 2025). The lignocellulosic fraction of olive pomace therefore represents a promising precursor for producing functional carbonaceous materials (Enaime *et al.* 2024). Biochar has attracted considerable interest as soil amendments because of its potential contributions to soil structure, water retention, and interactions with nutrients and organic compounds (Abdelfattah and Mostafa 2024).

Low-temperature chemical treatment and thermal conversion provide a potential pathway for converting olive pomace into functional carbonaceous materials while potentially reducing the thermal requirements associated with conventional high-temperature carbonization and activation processes. Recent studies have demonstrated the feasibility of producing functional carbonaceous materials from olive pomace through relatively mild thermal conversion and chemical activation (Deniz *et al.* 2022; Chafi *et al.* 2025; Alouiz *et al*. 2025). Their porous structure and oxygen-containing surface functionalities may facilitate water confinement and interactions with hydrophilic biopolymer matrices. The successful incorporation of carbonaceous materials into pectin-based porous structures further supports the potential of biochar–pectin combinations for developing functional composite materials (Wang *et al.* 2021).

Combining pectin hydrogels with biochar may therefore provide complementary functionality: the hydrophilic polymer network promotes water uptake and retention, whereas the bichar phase can provide additional pore domains and surface functionalities for interaction with the polymer matrix. Such integration provides a rational basis for developing bio-based composites for agricultural moisture management (Kanagalakshmi *et al*. 2024; Abdelfattah and Mostafa 2024).

Although previous studies have investigated pectin-based hydrogels for agricultural applications and biochar derived from agricultural residues separately, their integration within a unified olive pomace valorization pathway remains comparatively underexplored. The combined recovery of pectin and production of biochar material from olive pomace offers an opportunity to maximize resource utilization by converting different fractions of the same agro-industrial residue into complementary functional components. Integrating the hydrophilic and Ca^{2+}-cross linkable characteristics of pectin with the porous and surface-functional properties of olive pomace-derived biochar may provide complementary functionality for water uptake, retention, and structural stabilization. Such an integrated approach is consistent with circular-bioeconomy strategies aimed at converting olive-processing residues into value-added functional materials (Sun *et al.* 2025; Abdelfattah and Mostafa 2024).

Economic and cost assessment provides an important framework for evaluating the potential feasibility and scale-up of value-added products derived from olive pomace, addressing an important aspect of agricultural waste valorization (Morim *et al.* 2025; Alrowais *et al.* 2026). Recent studies have further highlighted the economic potential of integrated, multi-product biorefinery approaches, in which multiple value-added products are recovered from a single biomass feedstock, compared with conventional single-product valorization pathways (Prado-Acebo *et al*. 2024; Lamanna *et al*. 2026).

Accordingly, this study aimed to develop a biochar–pectin gel composite (BPGC) through an integrated olive pomace valorization pathway and evaluate its potential as a bio-based water-retaining soil amendment. The individual components and resulting composite were characterized in terms of their physicochemical, structural, and textural properties, followed by evaluation of water-holding capacity, moisture-retention behavior, microbial compatibility, seed germination, seedling development, and associated enzymatic responses. In addition, a preliminary economic and cost assessment was conducted to evaluate the economic potential of BPGC production. By integrating resource recovery, functional material development, biological evaluation, and preliminary economic assessment, the study provides a multidimensional framework for evaluating BPGC for water-scarce agricultural systems.

MATERIALS AND METHODS

Experimental Design

Figure 1 presents the flowchart of the current study. It provides an overview of the experimental and evaluation framework used in the study, illustrating how olive pomace was converted from a raw waste material into a safe-applicable BPGC and value-added products for sustainable agricultural applications. Raw olive pomace was characterized by chemical analysis and pectin extraction, including acidic (pH 1.8) and basic (pH 12.0) conditions.

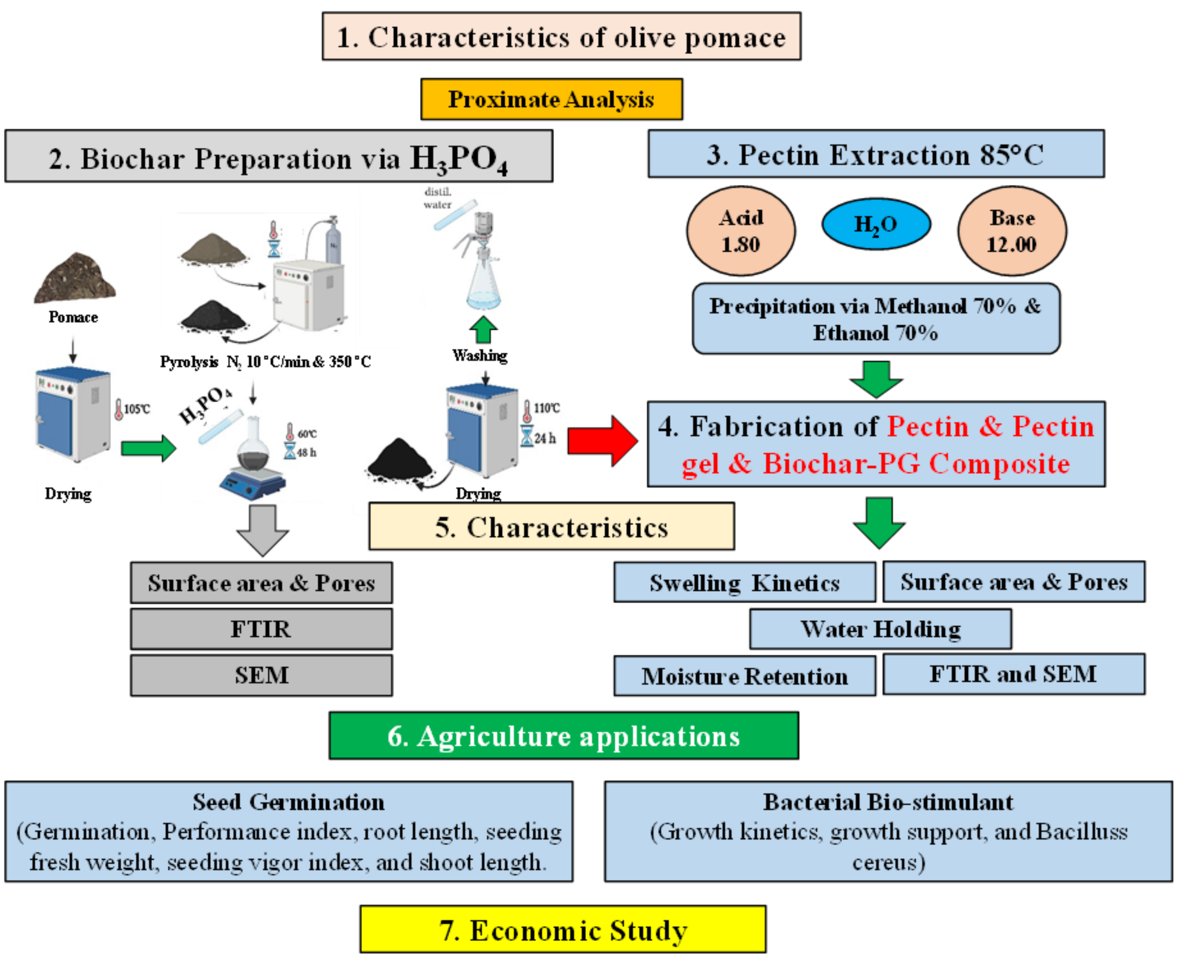

Fig. 1. Methodology flowchart of the current study

The remaining olive pomace was used to produce biochar. The process included drying the pomace, chemical impregnation with H_3PO_4, thermal treatment at 350 °C under nitrogen flow, followed by washing and drying. The biochar and the extracted pectin were characterized using several techniques, including surface area and pore structure analyses. Preparation of the BPGC was subsequently prepared and evaluated for water-holding capacity, swelling kinetics, and moisture retention. Finally, the effect of different pectin formulations (pectin, pectin gel, and BPGC) on seed germination and microbial growth inhibition were assessed.

Raw Material Source and Preparation

Olive pomace (a mixture derived from two- phase and three- phase extraction systems) was obtained from traditional olive oil manufacturing facilities and transported to the laboratory within one hour of collection. The pomace was stored at −18 °C for 12 h. It was dried in a press dryer at 60 °C for 16 h to reach a final moisture content of 6%. Dried pomace was ground to a fine powder at size 60 mesh, and the powder obtained was stored in zip-lock freezer bags (low- density polyethylene) under dry conditions for further use.

All the chemicals and reagents used were obtained from HiMedia Laboratories. Standard was supplied by Sigma Chemicals Co (Sigma Aldrich, India). The proximate composition, including crude protein, total fats, moisture content, total ash, and fibers (Horwitz and Latimer 2006). The carbohydrate content of the tested sample was determined by difference using the computation difference system (Horwitz and Latimer 2006) as follows:

$$\text{Carbohydrate (\%)} = 100 - [\text{Fat (\%)} + \text{Ash (\%)} + \text{Protein (\%)}] \quad (1)$$

Extraction of Pectin from Olive Pomace

Pectin extraction was performed by aqueous extraction under controlled acidic, neutral, and alkaline conditions according to Ali *et al.* (2025), with some modifications. Acidic conditions are commonly employed for pectin extraction because they facilitate pectin solubilization and recovery from plant matrices (Ali *et al.* 2025; Hosseini *et al.* 2016). Three separate and independent extraction experiments were conducted at pH 1.8, 7.0, and 12.0 using independent olive pomace samples, to systematically evaluate the effects of acidic, neutral, and alkaline conditions on pectin recovery. For each extraction, 50 g of dried olive pomace was dispersed in 1500 mL of distilled water, corresponding to a liquid-to-solid ratio (LSR) of 30 mL/g. The pH was adjusted to the desired value using HCl under acidic conditions and NaOH under alkaline conditions, while the neutral treatment was maintained at pH 7.0. Each mixture was heated at 85 °C for 2 h under mechanical stirring at 50 rpm.

After extraction, the mixture was cooled to room temperature and centrifuged at 5000 rpm for 15 min to separate the liquid extract from the residual solids. Pectin was subsequently precipitated by adding two volumes of either 95% ethanol or 95% methanol to the recovered supernatant, followed by overnight incubation at 4 °C. The precipitated pectin was collected by filtration, washed twice with 70% ethanol, and subsequently with absolute ethanol. The recovered pectin was dried at 40 °C for 24 h, ground into a fine powder, and stored in a desiccator until further analysis. Pectin yield was determined gravimetrically as the percentage of recovered dry pectin relative to the initial dry mass of olive pomace (Hosseini *et al.* 2016).

Determination of degree of pectin methyl esterification

FTIR spectroscopy was conducted to determine the degree of methyl esterification (DM) of the extracted pectin. The relative absorbance of the esterified and non-esterified carboxyl-group bands was used for the determination, providing a semi-quantitative assessment of pectin esterification (Muñoz-Almagro *et al.* 2019). The samples were ground in an agate mortar for proper homogenization before analysis. Spectra were recorded using an FTIR spectrophotometer (PerkinElmer, USA) across the range 400 to 4000 cm^{-1}. The DM was calculated from the relative absorbance of the bands identified at approximately 1740 cm^{-1}, corresponding to esterified carboxyl groups, and 1644 cm^{-1}, associated with ionized carboxylate groups, as follows:

$$DM\ (\%) = (A_{1740} / (A_{1740} + A_{1644})) \times 100 \quad (2)$$

Preparation of H_3PO_4 Treated Olive Pomace Biochar

The primary solid by-product of olive oil extraction was collected from a local olive-processing facility in the Al-Jouf Region, Saudi Arabia. It was then repeatedly washed with distilled water to remove impurities and subsequently dried. Chemical treatment was performed by impregnating 100 g of the dried olive pomace with phosphoric acid (H_3PO_4) at a weight ratio of 1:3 (pomace:H_3PO_4), followed by thorough mixing to ensure uniform penetration of H_3PO_4 (Abdel Daiem *et al.* 2019; Alrowais *et al.* 2026). The saturated samples were then thermally treated at 350 °C for 30 min and washed with distilled water until the filtrate reached a pH of around 6. Finally, the resulting biochar was dried at 105 °C for 24 h and stored in airtight containers for subsequent use.

Preparing of Pectin Gel Beads

Approximately 100 mL of 5% pectin solution, prepared by resuspension of 5 g of pectin in 95 mL of distilled water, was added dropwise into a bath filled with cold (thermostatic at 4 to 5 ºC) 20% $CaCl_2$ solution in 50% ethanol by pumping through a capillary (inner diameter of 1.0 mm) using a peristaltic pump. The spherical pectin hydrogel beads were incubated at 4 to 5 °C for 12 h in the same solution. Excess of $CaCl_2$ was washed with 100 mL portions of distilled water 3 to 5 times on a sieve (1.0 mm mesh), kept in 1 L of distilled water for at least 12 h at 4 to 5 ºC, and filtered. The procedure was adapted from previously reported pectin bead preparation method (Mata *et al.* 2009).

Preparation of BPGC Beads

Extracted pectin powder was dissolved in distilled water (3% w/v) at 60 °C under continuous stirring for 2 h. Biochar was dispersed independently in distilled water by ultrasonication (40 kHz, 30 min) to ensure uniform dispersion. The biochar loading was set at 10% (w/w), relative to the dry weight of pectin, based on previously reported polymer– carbon composite formulations composite formulations (Khoder *et al.* 2009) and preliminary formulation trials aimed at achieving homogeneous biochar dispersion and stable composite formation. The biochar suspension was also added dropwise to the pectin solution under vigorous stirring. The mixture was stirred for 2 h to ensure homogeneous distribution. Composite hydrogel beads were prepared by ionic crosslinking using the dropping method. The biochar-pectin mixture was loaded into a syringe and extruded dropwise into 500 mL of 20% (w/v) $CaCl_2$ solution under gentle stirring. The distance between the needle tip and the surface of crosslinking solution was maintained at 10 cm to ensure uniform spherical bead formation. The beads were allowed to crosslink in the $CaCl_2$

solution for 2 h at room temperature, collected by filtration, washed thoroughly with distilled water to remove residual surface $CaCl_2$, and then stored in distilled water at 4 °C for immediate testing or dried at 40 °C for 24 h for dry-state characterization (Farrukh *et al.* 2025) with some modifications.

The pectin extraction temperature and duration (85 °C and 2 h, respectively) were adapted from established extraction protocols (Ali *et al.* 2025; Hosseini *et al.* 2016), while the effects of extraction pH (1.8, 7.0, and 12.0) and precipitating alcohol (ethanol or methanol) were experimentally evaluated in the present study. The biochar preparation parameters, including an olive pomace to H_3PO_4 impregnation ratio of 1:3 (w/w) and thermal treatment at 350 °C for 30 min, were selected based on previously established procedures for olive pomace-derived carbonaceous materials (Abdel Daiem *et al.* 2019). The 10% biochar loading was selected based on previously reported polymer–carbon composite formulations and preliminary formulation trials to achieve homogeneous dispersion and stable bead formation. The selected conditions were based on literature-guided protocols, experimental screening of the extraction conditions, and preliminary composite formulation trials.

Characterization of Pectin, Pectin Gel, Biochar, and BPGC

Surface functional groups of pectin, pectin gel, biochar, and BPGC were verified through Fourier transform infrared (FTIR) spectroscopy using a PerkinElmer Spectrometer (PerkinElmer Inc., Waltham, MA, USA) over the wavenumber range of 4000 to 550 cm^{-1}. Surface morphology and microstructural features were studied through scanning electron microscopy (SEM) using a JEOL JSM-6510LV (JEOL Ltd., Tokyo, Japan). Textural properties, including specific surface area, pore diameter, and pore volume, were measured using Brunauer–Emmett–Teller (BET) adsorption analysis performed on a Micromeritics ASAP 2020 surface area and porosity analyzer (Micromeritics Instrument Corp., Norcross, GA, USA).

Evaluation of Water Retention Properties

Swelling ratio

Swelling experiments were conducted gravimetrically in distilled water. Pre-weighed dry samples (100 mg) were immersed in 50 mL of distilled water at 25 °C and allowed to swell. At designated time intervals (10, 20, 30, 60, 120, and 240 min), samples were gently removed, excess surface water was carefully removed using filter paper, and the samples were weighed. The swelling rate (SR) was calculated by the following Eq. 3,

$$SR\ (\%) = ((W_t - W_d) / W_d) \times 100 \quad (3)$$

where W_t is the sample weight at a time t, and W_d is the initial dry weight in grams (Neha *et al.* 2019). Equilibrium swelling was considered achieved when three successive measures showed a change of less than 2%. All measurements were performed in triplicate.

Water holding capacity (WHC)

The WHC of the tested samples was measured by adding 2 mL of water to 100 mg of sample, shaking for 24 h, and centrifuging at 4500 × g for 30 min. WHC was measured as the volume of water retained for each gram of dry sample (mL/g) (Fuentes-Alventosa *et al.* 2009).

Moisture retention under evaporative conditions

Moisture retention kinetics were estimated by observing water loss from completely swollen samples under controlled evaporative conditions. Samples equalized in distilled water were transferred to open Petri dishes and placed in an environmental chamber maintained at 25 °C and 45% relative moisture. Sample weights were recorded at 10, 20, 30, 60, 120, and 240 min, and moisture retention (MR) was calculated as,

$$MR\ (\%) = (W_t - W_d) / (W_0 - W_d)) \times 100 \quad (4)$$

where W_t is the sample weight at time t, W_d is the dry weight, and W_0 is the initial swelling weight at time zero (Liu *et al.* 2025).

Biocompatibility Assessment

Microbial growth test

The examined strain, *Bacillus Cereus*., was isolated from natural soil (Bashan and de-Bashan 2010). Pectin, pectin gel, and BPGC were tested at concentrations of 1%, 3%, and 6% (w/v). Each treatment medium was inoculated at 1% (v/v) with an overnight bacterial culture containing approximately 10^8 CFU/mL. Optical density (OD) at 660 nm was estimated for a 24 h period at 37 °C (1 h intervals) using a SPECTROstar Nano microplate reader (BMG LABTECH GmbH, Ortenberg, Germany), with the increase in OD_{660} used as an indicator of bacterial growth. A positive control (inoculated medium without pectin, pectin gel, or BPGC) and a negative control (uninoculated medium) were also used for comparison. Each condition was examined in triplicate. The growth inhibition percentage was measured using the following,

$$\text{Inhibition}\ (\%) = ((OD_{control} - OD_{treatment}) / OD_{control}) \times 100 \quad (5)$$

where *ODcontrol* represents the OD_{660} of the positive bacterial control, and *ODtreatment* represents the OD_{660} of the bacterial culture in the presence of the tested material.

Germination Bioassay and Phytotoxicity Assessment

The phytotoxicity of pectin, pectin gel, and BPGC were examined using tomato seeds (*Solanum lycopersicum* var. cerasiforme) following the protocol established by ISTA (ISTA 2020). Pectin, pectin gel, and BPGC (1.0 g) were separately soaked in 50 mL of distilled water for 48 h at 25 °C to prepare aqueous extracts. Tomato seeds were surface-sterilized with 1% sodium hypochlorite for 5 min, thoroughly irrigated with sterile distilled water, and placed on sterile cotton in Petri dishes containing 5 mL of each extract or sterile distilled water as a control. All petri dishes were incubated at 25 °C in the dark for 7 days. Germination percentage, root length, and shoot length were measured (Cao and Li 2021).

Preliminary Techno-Economic Assessment

A preliminary deterministic techno-economic assessment (TEA) was conducted to evaluate the potential economic feasibility of BPGC production, following the general framework of Asare *et al.* (2026), with modifications to reflect the BPGC production process. The assessment considered a production capacity of 200 t/year and an operating period of 300 days/year, corresponding to an average production rate of approximately 667 kg/day. A 10-year project lifetime and a 10% discount rate were assumed.

The assessment included the major cost components associated with BPGC production, including olive pomace feedstock, chemical reagents (H_3PO_4, $CaCl_2$, and ethanol/methanol), process water, and energy consumption associated with drying and thermal processing, labor, and capital expenditure. Olive pomace was valued at approximately \$20/t, broadly consistent with values reported for olive pomace in previous valorization studies (Parascanu *et al.* 2018), while the BPGC selling price was assumed to be \$3.00/kg. Economic performance was evaluated using unit production cost, gross margin, net present value (NPV), internal rate of return (IRR), and simple payback period. The deterministic assessment provides preliminary economic estimates under the adopted technical and market assumptions; sensitivity analysis and pilot-scale validation are required before commercial feasibility can be established.

Statistical Analysis

Statistical analyses and data presentation were conducted using SPSS version 27 and Microsoft Excel 365. All experiments were performed in triplicate (n = 3 independent experimental replicates), and the results are expressed as mean ± standard deviation (SD) to describe variability among replicates. The experimental unit was defined as an independently prepared sample or treatment replicate. Statistical differences among treatments were evaluated using one-way analysis of variance (ANOVA), followed by Tukey's HSD post-hoc test for multiple comparisons, with statistical significance set at $P < 0.05$.

RESULTS AND DISCUSSION

Olive Pomace Composition and Pectin Recovery

Chemical composition of olive pomace

The proximate analysis of olive pomace displayed in Table 1 indicated a heterogeneous composition, characterized by a high moisture content (49.3%, wet basis) and a high carbohydrate content (70.0% DW), consistent with the abundance of structural polysaccharides in olive-derived residues. The protein (8.87% DW) and lipids (10.74% DW) were substantial and showed some variation compared with values reported in previous studies (El-Shatoury *et al.* 2014; Alimenti *et al.* 2023). Such differences are expected because the chemical composition of olive pomace can vary considerably depending on olive cultivar, growing conditions, and oil-extraction technology (Guerboub *et al.* 2025). The relatively high carbohydrate content observed in the present study further supports the suitability of olive pomace as a feedstock for the recovery of pectin and the production of bio-based materials.

Table 1. Chemical Composition of Olive Pomace Powder

Component	Mean ± SD
Moisture content (% wet basis)	49.32 ± 4.24
Protein (%DW)	8.87 ± 0.21
Lipids (%DW)	10.74 ± 0.33
Carbohydrates (%DW)	70.02 ± 2.64
Fiber (%DW)	29.59 ± 0.77
Ash (%DW)	5.12 ± 0.78

Note: Moisture content is reported on a wet-weight basis, whereas the other components are expressed on a dry-weight (% DW) basis; the crude fiber fraction contains structural carbohydrates as well as lignin; and the ash value may be subject to minor variation due to mineral/crystal transformations and associated water loss during ashing at 550 °C.

Effect of extraction conditions on pectin yield

As shown in Table 2, both the extraction pH and the type of precipitating alcohol markedly influenced the pectin recovery yield of olive pomace pectin. Methanol consistently resulted in higher pectin yields than ethanol, which may be related to differences in solvent polarity and precipitation efficiency resulting from reduced pectin solubility and disrupting the hydration environment surrounding the polymer chains (Pattarapisitporn and Noma 2025). The highest pectin yield (11.8%) was obtained using acid-assisted extraction at pH 1.8 and 85 °C, followed by methanol precipitation. Under controlled acidic conditions, protonation of pectic carboxylate groups and disruption of interactions between pectin and other cell-wall constituents can facilitate the release and solubilization of pectic polysaccharides. Mild acid-assisted extraction may also induce partial modification of pectin, including changes in esterification and molecular structure, depending on pH, temperature, and extraction duration (Ciriminna *et al.* 2016; Freitas *et al.* 2021). In the present study, the extracted pectin exhibited a low degree of methyl esterification, supporting its suitability for subsequent Ca^{2+}-mediated "egg-box" crosslinking.

Conversely, alkaline extraction at pH 12.0 resulted in lower pectin yields (7.34 to 8.61%). Strong alkaline conditions can promote β-elimination and other degradation reactions in pectic polysaccharides, resulting in chain cleavage and the formation of lower-molecular-weight fractions that may be less efficiently recovered by alcohol precipitation (Adetunji *et al.* 2017). The advantage of methanol over ethanol was particularly evident under acidic extraction conditions, where the difference in recovery yield reached 3.68 percentage points. This observation may reflect differences in solvent polarity and precipitation behavior toward solubilized pectic fractions (Prasertsit *et al.* 2021). Overall, the results identify acid-assisted extraction followed by methanol precipitation as the most effective condition among those evaluated in the present study.

Table 2. Effect of Extraction Conditions on Pectin Yield (% DW)

Extraction/Treatment	Ethanol Pectin Yield (%)	Methanol Pectin Yield (%)
Neutral solution	9.72 ± 0.47	10.23 ± 0.27
Basic solution	7.34 ± 0.31	8.61 ± 0.42
Acidic solution	8.10 ± 0.50	11.78 ± 0.68

Physiochemical and Structural Characterization

FTIR analysis

FTIR spectroscopy presented in Fig. 2 confirmed the integrity of olive pomace pectin structure. It showed a broad O–H stretching band at 3562 to 3333 cm^{-1} and C–H vibrations at 2928 to 2860 cm^{-1}. The diagnostic areas (1800 to 1200 cm^{-1}) revealed key peaks at 1740 cm^{-1} (for esterified C=O) and 1644 cm^{-1} (for free -COO), reflecting the esterification characteristics of the extracted pectin (Manrique and Lajolo 2002; Černá *et al.* 2003; Abdel Daiem *et al.* 2021). The band at 1406 cm^{-1} was attributed to symmetric carboxylate stretching, while those at 1247 and 1073 cm^{-1} were associated with C–O and C–O–C vibrations of the polysaccharide backbone. Bands at approximately 892 and 808 cm^{-1} were also observed in the fingerprint region, further supporting the characteristic polysaccharide structure of the extracted pectin (Kačuráková *et al.* 2000). Overall, these spectral features support the successful extraction of pectin with preservation of its characteristic functional groups (Guerboub *et al.* 2025).

The calculated DM of 38.2% classifies the extracted pectin as low-methoxy (LM) pectin (DM < 50%) (Braccini and Pérez 2001). Although the ester carbonyl band at 1740 cm^{-1} appears visually prominent, its intensity alone should not be interpreted as evidence of a high degree of methyl esterification. The simultaneous presence of prominent carboxylate-associated bands at 1644 and 1406 cm^{-1} indicates a considerable proportion of non-esterified galacturonic acid residues. Therefore, the overall FTIR profile supports the partially de-esterified, low-methoxy character of the extracted pectin (Dranca and Oroian 2018). This low-methoxy character facilitates Ca^{2+}-mediated gelation, supporting its suitability for biodegradable hydrogel formation (Said *et al.* 2023).

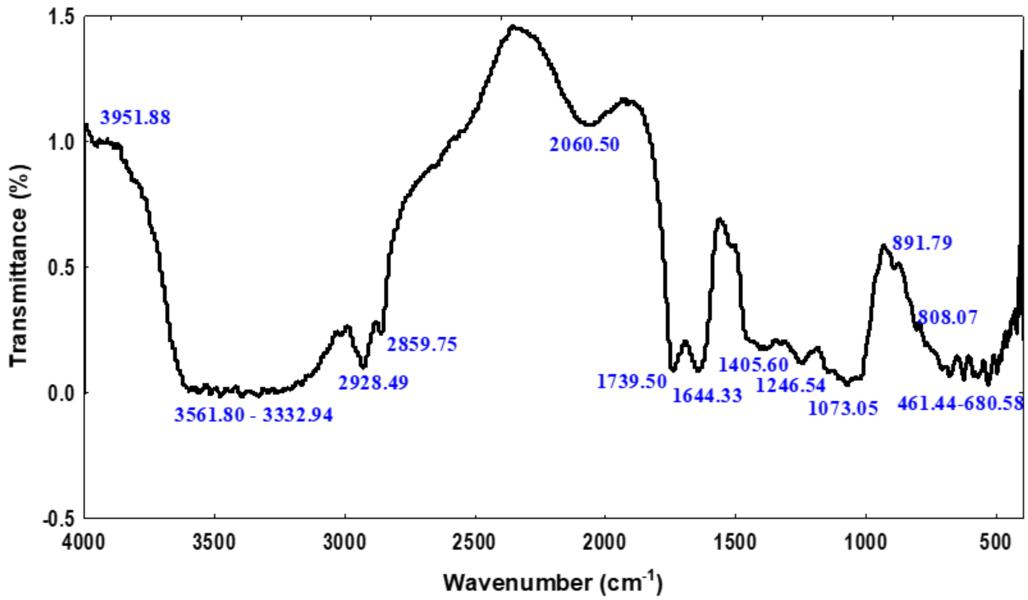

Fig. 2. FTIR profile of extracted pectin

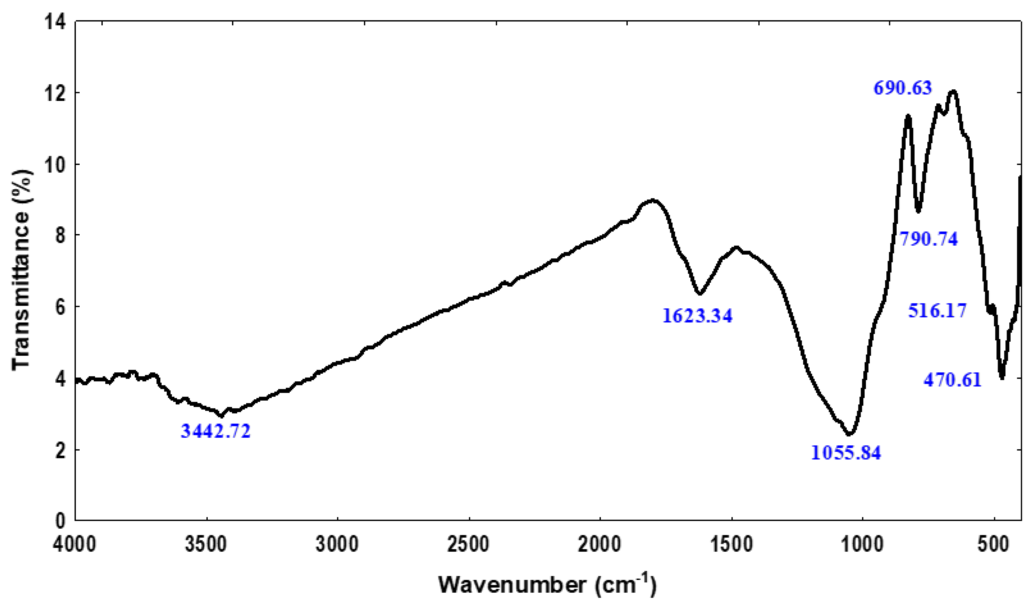

Fig. 3. FTIR profile of biochar

The FTIR analysis (Fig. 3) of biochar showed a carbon matrix exhibiting aromatic and oxygenated functional groups, characterized by broad O–H stretching at 3443 cm^{-1} and a prominent aromatic C=C band at 1623 cm^{-1} (Rani *et al.* 2022). The band at 1056 cm^{-1} was assigned to C–O stretching of oxygen-containing surface groups, which contribute to surface polarity, while lower-frequency bands at approximately 791, 691, 516, and 471 cm^{-1} may be associated with aromatic C–H out-of-plane and skeletal vibrations, as well as possible residual inorganic constituents (Abdel daiem *et al.* 2020, 2019). These oxygen-containing groups (O–H and C–O) can promote hydrogen bonding and other non-covalent interactions, facilitating interactions between the biochar surface and surrounding molecules or polymeric components (Alrowais *et al.* 2026). The development of the aromatic carbon framework together with the retention of oxygen-containing surface functionalities is consistent with the structural modification induced by phosphoric acid treatment (Abdel Daiem *et al.* 2019; Ibeh *et al.* 2019).

The FTIR spectrum of the pectin gel (Fig. 4) supported the formation of an ionically cross-linked pectin network through interactions between carboxylate groups ($–COO^-$) and Ca^{2+} ions. A prominent carboxylate-associated band was observed at 1646 cm^{-1}, together with a band at 1391 cm^{-1}, consistent with asymmetric and symmetric COO^- vibrations involved in Ca^{2+}-mediated crosslinking. The absence of a prominent ester-carbonyl band around 1740 cm^{-1}, compared with the extracted pectin spectrum, further supports the predominance of carboxylate groups available for ionic interaction and formation of the characteristic “egg-box” network. The O–H-related region extending toward 3571 cm^{-1} is consistent with hydrogen-bonded hydroxyl groups within the polysaccharide network. The structural integrity of the pectin backbone is further supported by C–O–C and C–O stretching vibrations at 1200, 1111, and 1058 cm^{-1} (Said *et al.* 2023; Vicente *et al.* 2026).

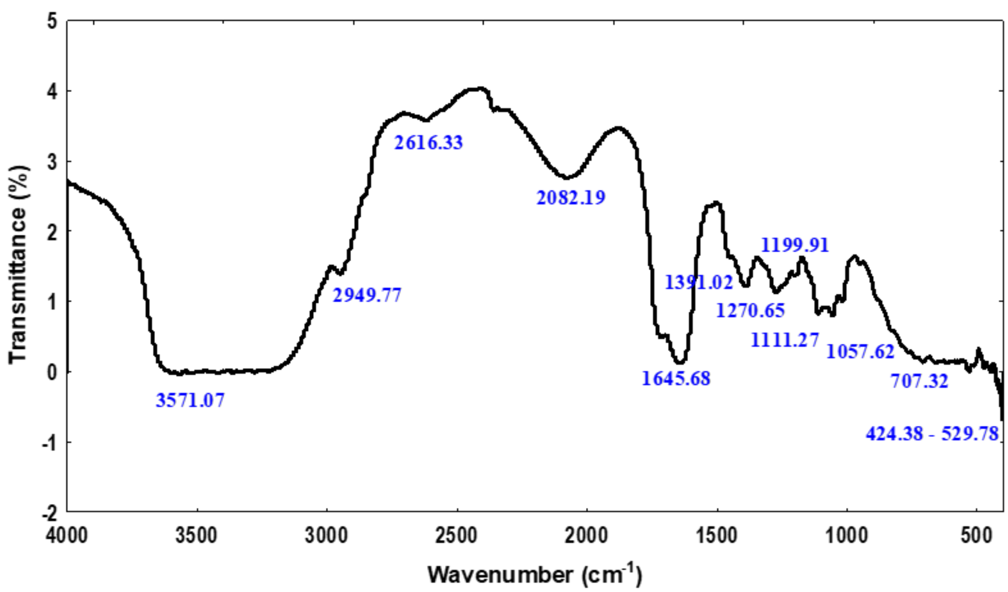

Fig. 4. FTIR profile of pectin gel

The FTIR spectrum of the BPGC (Fig. 5) supported the integration of biochar within the Ca^{2+}-crosslinked pectin matrix. The bands observed at 1741 and 1635 cm^{-1} were assigned to ester carbonyl (C=O) and carboxylate (COO^-) groups, respectively, while the band at 1418 cm^{-1} was associated with symmetric carboxylate stretching, supporting Ca^{2+}-mediated interactions within the pectin network. Hydrogen bonding within the composite was indicated by the broad O–H stretching band at 3411 cm⁻¹ (Said *et al.* 2023). The polysaccharide structure was retained, as indicated by the strong C–O/C–O–C-related band at 1043 cm^{-1} (Vicente *et al.* 2026). Additional bands at 777, 556, and 518 cm^{-1} were observed following composite formation and may reflect low-frequency skeletal vibrations and structural changes associated with biochar incorporation into the pectin matrix.

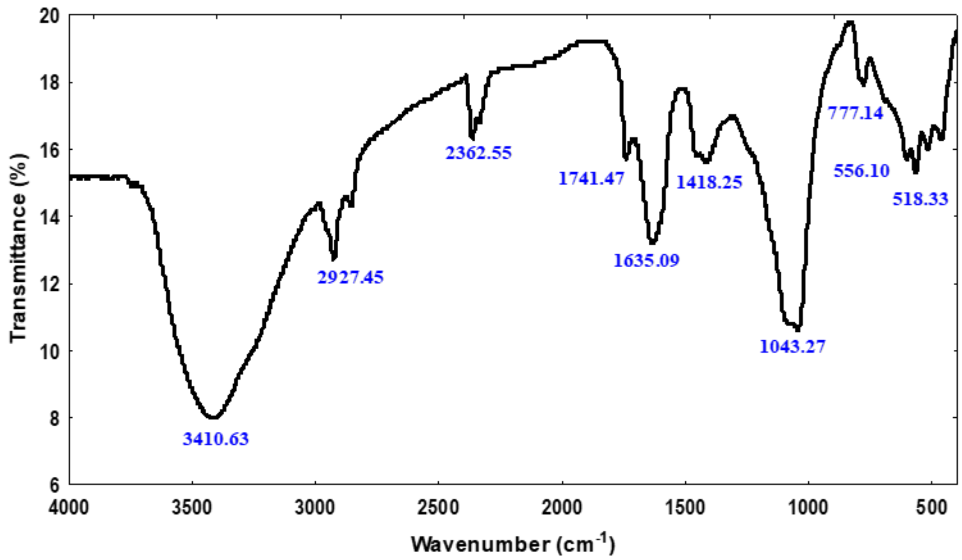

Fig. 5. FTIR profile of BPGC

BET analysis and textural characterization

The textural characteristics of the isolated olive pomace pectin were evaluated using N_2 adsorption–desorption isotherms at 77 K. The analysis revealed a BET specific surface area of 28 m^2/g, indicating a relatively low N_2-accessible surface area. This is consistent with the compact macromolecular nature of pectin. A low BET C constant of 2.25 was observed, indicating weak nitrogen–surface interactions typical of Type III isotherm behavior in organic biopolymers (Adamczak *et al.* 2016). Barrett–Joyner–Halenda (BJH) analysis yielded a cumulative pore volume of 0.025 cm^3/g and a mean pore radius of 1.92 nm, indicating the presence of pores within the mesoporous size range. Density functional theory (DFT) modeling further revealed a bimodal pore-size distribution with peaks at 1.01 and 2.94 nm. These textural characteristics may reflect the spatial organization of galacturonic acid-rich polysaccharide chains within the dried pectin matrix (Bermúdez-Oria *et al.* 2021), supporting its potential application as a bioactive carrier in agricultural systems (Millán-Linares *et al.* 2021).

The biochar was also characterized by N_2 adsorption–desorption analysis at 77 K. It exhibited a predominantly mesoporous structure, with a mean pore diameter of 9.56 nm and a distribution peak at 28.9 nm. It showed a BET surface area of 24 m^2/g and a total pore volume of 0.11 cm^3/g, reflecting moderate pore development under the relatively mild thermal treatment at 350 °C. The observed textural characteristics are consistent with the relatively mild preparation conditions used for the olive pomace biochar. The hysteresis loop observed at $P/P_0 > 0.8$ indicated capillary condensation within larger mesopores, while a BJH pore area of 14 m^2/g and substantial N_2 uptake at high relative pressures suggested the additional presence of larger pore domains and/or interparticle voids. For the intended soil-amendment application, maximizing BET surface area was not the primary objective; rather, the low-temperature preparation route was intended to balance pore development, surface functionality, and processing severity.

Following Ca^{2+}-induced gelation, the pectin gel exhibited a lower BET surface area of 19 m²/g compared with isolated pectin (~28 m²/g), which is consistent with the formation of a more compact interconnected network. According to the "egg-box" model, Ca^{2+} coordination with carboxylate groups of adjacent galacturonic acid residues promotes chain association and reduce the surface accessible to N_2 in the dried gel. The gel exhibited a BET C constant of 2.12, cumulative pore volume of 0.015 cm³/g, and mean pore radius of 1.92 nm, while DFT analysis retained peaks at 1.01 and 2.94 nm (Adamczak *et al.* 2016; Bermúdez-Oria *et al*. 2021; Millán-Linares *et al.* 2021).

The BPGC exhibited a further decrease in BET specific surface area to 9.9 m²/g compared with isolated pectin (~28 m²/g), pectin gel (~19 m²/g), and biochar (~24 m²/g). This reduction can be attributed to coating of biochar particles by pectin chains, partial blockage of N_2-accessible pores, and structural shrinkage during conversion of the hydrated gel to the dried state (Adamczak *et al.* 2016). Nevertheless, DFT analysis showed preservation of distinct pore domains, with peaks at 1.01 and 2.94 nm. Because similar pore-size features were also observed in the pectin-based materials, these peaks cannot be assigned exclusively to a single phase but may reflect contributions from both the porous biochar phase and the Ca^{2+}-crosslinked pectin network. This would be consistent with the structural characteristics reported for biomass-derived carbonaceous materials and ionically crosslinked pectin systems (Deniz *et al.* 2022).

Thus, although composite formation reduced the dry-state BET surface area, the coexistence of biochar-derived pores, interstitial spaces, and hydrophilic functional groups provides a heterogeneous pore–polymer architecture. Importantly, the relatively low dry-state BET surface area of BPGC does not necessarily indicate poor water-retention performance because N_2 physisorption characterizes the accessible surface of the dried material, whereas water retention occurs within a hydrated polymer network. Upon hydration, oxygen-containing functional groups may promote water interactions, while porous domains and biochar–polymer interfacial spaces contribute to capillary confinement. Together with Ca^{2+}-mediated pectin crosslinking, these characteristics provide a plausible structural basis for the observed high water-holding capacity (97.9%) despite the relatively low dry-state BET surface area (Wang *et al.* 2021; Deniz *et al.* 2022; Hou *et al.* 2022; Said *et al.* 2023).

SEM analysis

The SEM micrographs of the pectin gel in Fig. 6a showed a smooth, dense, and continuous polymeric matrix with minimal notable porosity. This microstructure is consistent with previous studies on pectin gels, which have shown homogeneous networks with compact structures and limited pore formation (Walkenström *et al.* 2003; Kyomugasho *et al.* 2016). Pure pectin networks have been reported to exhibit thinner strands and smaller pore sizes, reflecting the relatively uniform organization of the polymer network (Walkenström *et al.* 2003). Consistent with these observations, the pectin gel in the present study exhibited a dense and relatively homogeneous morphology without visible particulate or large porous structures. The continuity of the polymeric matrix indicates the formation of a compact gel network, whose structural organization is primarily governed by polymer-chain interactions and hydrogen bonding (Kyomugasho *et al.* 2016).

The SEM micrograph of biochar in Fig. 6b revealed a highly heterogeneous, fractured, and porous surface morphology consistent with H_3PO_4-treated biochar derived from lignocellulosic biomass. The surface is densely populated with irregular cavities, fissures, and granular aggregates, indicating the development of visible porous and fractured domains (Chafi *et al.* 2025). Numerous plate-like and rock-shaped carbon fragments were also observed, which may result from thermal decomposition and dehydration of the lignocellulosic components during carbonization and H_3PO_4 treatment (Deniz *et al.* 2022). These findings are in strong agreement with previous studies documenting rough, cracked, and porous morphologies for H_3PO_4-treated biomass-derived carbonaceous materials (Alouiz *et al.* 2025). Overall, the observed morphology confirms the development of a heterogeneous porous biochar structure suitable for incorporation into the pectin matrix.

SEM micrographs revealed distinct microstructural differences between the pectin gel (Fig. 6a) and the BPGC in (Fig. 6c), providing morphological evidence relevant to their different water-holding and moisture-retention behaviors. The pectin gel showed a smooth, dense, and continuous polymeric matrix *via* minimal porosity, consistent with prior notes that pure pectin gels form homogeneous, compact networks with limited pore structures when visualized by SEM (Kyomugasho *et al.* 2016). Pectin networks are composed of "thinner strands and smaller pore sizes" matching to composite, which has been referred to as the regular crosslinking density within the pectin gels (Walkenström *et al.* 2003). In contrast, BPGC exhibited a more heterogeneous and rough morphology, with biochar particles visibly embedded within the pectin matrix and the formation of irregular interfacial spaces and porous domains. Previous studies have similarly reported increased porosity following incorporation of carbonaceous particles into pectin-based matrices (Wang *et al.* 2021). Comparable pectin–carbon composites have also exhibited rougher and more interconnected porous structures than the corresponding pectin matrices, which may contribute to improved water confinement and retention (Kanagalakshmi *et al.* 2024). These morphological differences, together with the BET results, support the physical integration of biochar within the pectin matrix and the formation of a heterogeneous biochar–polymer architecture.

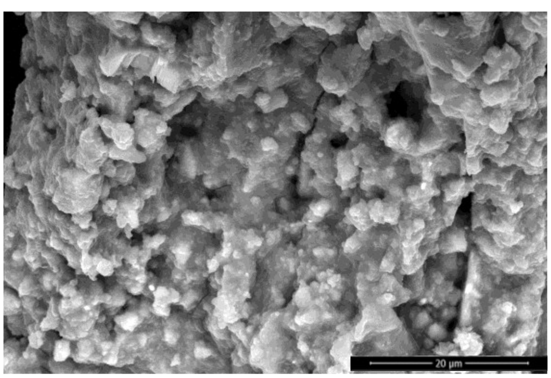

a)

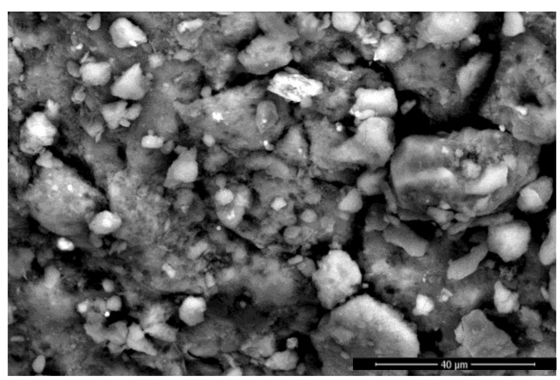

b)

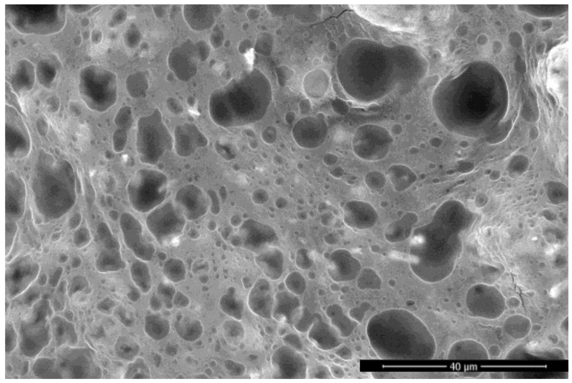

c)

Fig. 6. SEM analysis of a) pectin gel, b) Biochar, and c) BPGC

Interfacial interactions and composite structure validation

Complementary characterization analyses provide evidence for the physical integration and interfacial interactions of the biochar phase within the calcium-crosslinked pectin matrix of BPGC. FTIR analysis showed characteristic ester carbonyl and carboxylate bands at 1741 and 1635 cm^{-1}, respectively, together with a broad O–H stretching band at 3411 cm^{-1}. The carboxylate-associated band at 1418 cm^{-1} and the C–O/C–O–C-related band at 1043 cm^{-1} further reflected the chemical environment of the crosslinked polysaccharide matrix. Collectively, these spectral features are consistent with Ca^{2+}-mediated pectin crosslinking and suggest the contribution of hydrogen bonding and other non-covalent interactions between oxygen-containing functional groups of the biochar surface and the pectin matrix.

The interfacial integration is further supported by BET and morphological observations. The BET specific surface area decreased to 9.9 m^2/g in BPGC compared with approximately 28 m^2/g for isolated pectin and 19 m^2/g for the Ca^{2+}-crosslinked pectin gel. This reduction is consistent with partial coverage of biochar particles by pectin chains, partial blockage of N_2-accessible pores, and structural contraction of the polymer network during drying. SEM observations further showed biochar particles distributed within the pectin matrix and a heterogeneous morphology containing irregular interfacial and porous domains, consistent with the formation of an integrated composite structure. Functionally, this architecture restricted equilibrium swelling to approximately 160%, while BPGC maintained a high water-holding capacity of 97.9%, indicating that a lower swelling ratio does not necessarily imply poor water-holding performance. Instead, water retention may arise from the combined contributions of polymer hydration, Ca^{2+}-mediated network formation, hydrophilic surface interactions, and water confinement within porous and biochar–polymer interfacial domains.

Swelling and Water Retention Performance

Swelling behavior in distilled water

The swelling kinetics of pectin, pectin gel, and BPGC were examined in distilled water. The swelling ratios measured at different immersion times are presented in Fig. 7. The materials exhibited distinct swelling patterns reflecting differences in their structures. Pectin showed the highest and fastest swelling, reaching 121% within 10 min, followed by a rapid increase to 189% after 1 h and approximately 195% after 2 h. Significant differences among the early measurement periods indicated rapid initial swelling, which can be associated with the greater mobility and hydration of the hydrophilic polymer chains in non-crosslinked pectin (Einhorn-Stoll *et al.* 2016).

In contrast, the pectin gel showed significantly lower swelling than pectin at most measurement times, ranging from 104% at 10 min to 178% at 4 hours. Swelling increased more gradually during the first 3 h, consistent with the presence of Ca^{2+}-mediated crosslinks that restrict polymer-chain mobility and moderate network expansion (Said *et al.* 2023). Consistently, BPGC showed the lowest swelling at most measurement times. From 20 min, it was lower than both other treatments, which may be attributed to the incorporation of relatively rigid, non-swelling biochar particles that reduce the effective fraction of swellable pectin and physically constrain polymer-chain expansion. At 10 min, both the pectin gel and the composite were similar, but they diverged thereafter as the internal structure dominated. Equilibrium swelling followed the order pectin (195%) > pectin gel (178%) > BPGC (160%). The approximately 10% lower maximum swelling of BPGC relative to the pectin gel is consistent with reduced expansion of the polymer network following biochar incorporation. Thus, pectin exhibited rapid and extensive hydration, whereas Ca^{2+} crosslinking moderated swelling in the pectin gel, and biochar incorporation further limited the expansion of BPGC. This controlled swelling behavior, combined with its high water-holding capacity, may be advantageous for soil-moisture management applications where water retention rather than maximum volumetric expansion is desired (Sultana 2023).

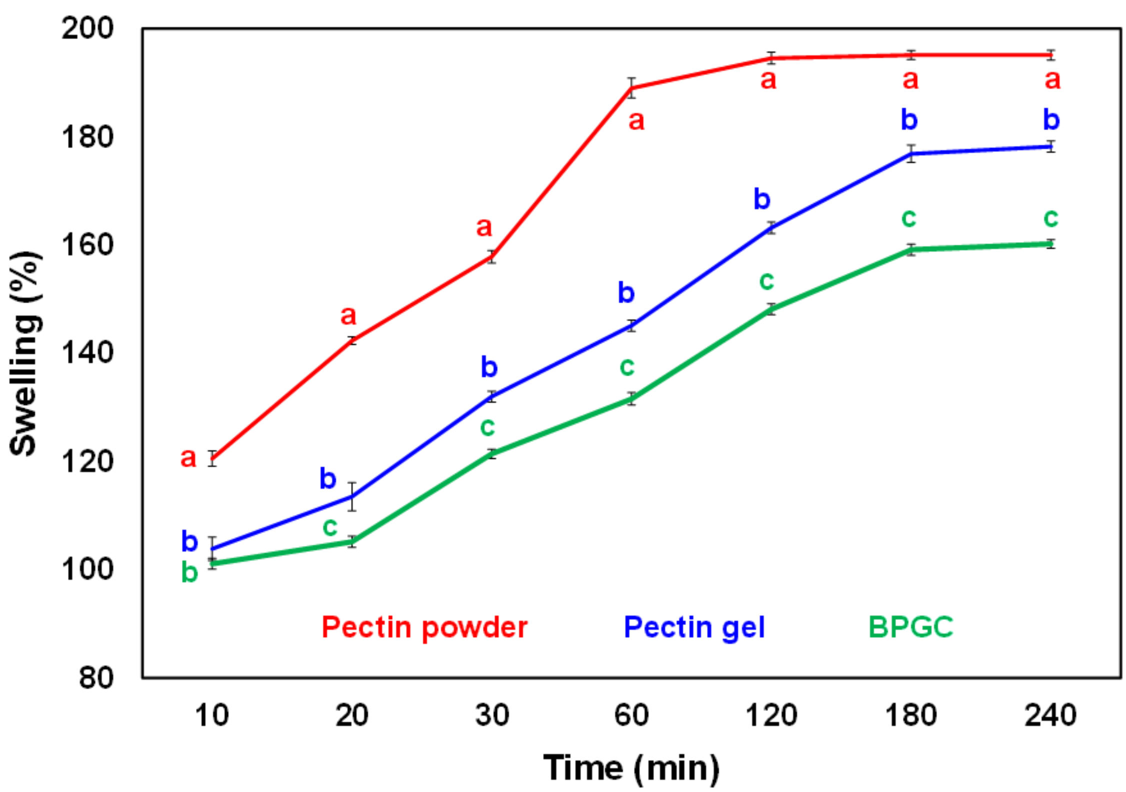

Fig. 7. Swelling behavior of pectin powder, pectin gel, and BPGC in distilled water. The values within the same treatment time and letter do not differ significantly at $P \leq 0.05$.

Moisture retention under evaporative conditions

The moisture retention kinetics of pectin, pectin gel, and BPGC reported in Fig. 8 revealed distinct differences in moisture retention among the three materials: Pectin revealed the lowest retention, dropping quickly from 81.1% at 10 min to 11.1% at 4 h, owing to the absence of a gel network that allows evaporation of free water. The pectin gel showed superior retention: 94.8% at 10 min and 36.6% at 4 h, indicating that the Ca^{2+}-crosslinked matrix improved water confinement and reduced moisture loss. BPGC exhibited the highest moisture retention throughout the evaluated period, retaining 60% of its initial water content after 4 h. This enhanced retention may result from the combined effects of the Ca^{2+}-crosslinked pectin network, water confinement within porous and biochar–polymer interfacial domains, and hydrogen bonding between water and oxygen-containing functional groups within the composite. Consequently, BPGC shows promising water-retention characteristics as a bio-based soil amendment for improving soil-moisture conservation, particularly under water-limited conditions (Soliman and Mansour 2024; Agbna and Zaidi 2025).

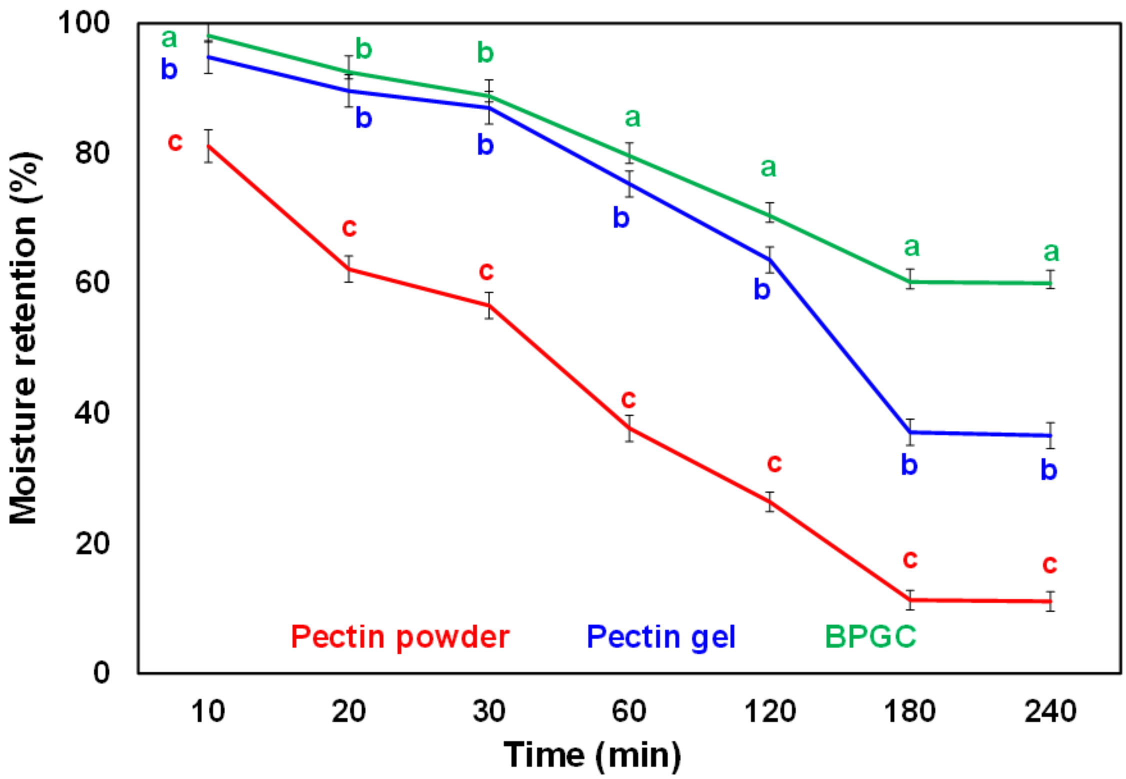

Fig. 8. Moisture retention kinetics of pectin, pectin gel, and BPGC over time. The values within the same treatment time and letter did not differ significantly at P ≤ 0.05.

Water holding capacity

Table 3 illustrates the differences in WHC among pectin, pectin gel, and BPGC. The non-gelled pectin exhibited the lowest WHC (31.2%), reflecting its lack of a crosslinked three-dimensional network capable of effectively retaining water under centrifugation. The presence of a calcium-cross linked pectin gel significantly enhanced the WHC to 44.1% as the three-dimensional gel network is effective at holding water (Sultana 2023). The highest WHC was observed for BPGC (97.9%), representing a substantial improvement over both pectin and pectin gel. This enhancement suggests a complementary contribution of the crosslinked pectin matrix and incorporated biochar. The pectin gel provides the primary cross-linked matrix, while the biochar particles act as a filler and for additional physical cross-linkage (Kabiri *et al.* 2011).

The enhanced water-holding capacity (97.9%) of BPGC can be attributed to the synergistic contribution of three complementary mechanisms: (i) hydrogen bonding between water molecules and abundant oxygen-containing functional groups (–COOH, –OH, and C=O) within the pectin–biochar matrix; (ii) water confinement within porous domains and biochar–polymer interfacial spaces; and (iii) physical confinement of water within the Ca^{2+}-mediated "egg-box" pectin network, which restricts polymer-chain mobility and limits rapid water loss (Das and Ghosh 2022). Incorporation of relatively rigid biochar particles within the ionically crosslinked biopolymer matrix further contributes to structural reinforcement and controlled polymer expansion. Consequently, BPGC combines a lower maximum observed swelling ratio (~160%) with substantially higher water-holding capacity (97.9%), indicating that restricted volumetric swelling can coexist with effective moisture storage. This complementary behavior highlights the potential of the biochar–pectin composite as a water-retaining amendment for agricultural applications (Shu *et al.* 2025).

The apparent contrast between the relatively low dry-state N_2 BET surface area of BPGC (9.9 m^2/g) and its high water-holding capacity (97.9%) highlights the fundamental difference between gas physisorption in a dried composite and water interactions within a hydrated polymer matrix. During drying, contraction of the pectin network and coating of the embedded biochar particles may partially mask or block N_2-accessible pores, thereby reducing the measured BET surface area. Upon hydration, however, abundant oxygen-containing functional groups, including –OH, C=O, and $–COO^-$ groups, can interact with water through hydrogen bonding and other polar interactions. DFT analysis further revealed a bimodal pore-size distribution with characteristic domains at approximately 1.01 and 2.94 nm, indicating the presence of nanoscale pore domains within the dried composite structure. Similar pore-size features were observed in the pectin-based materials. These pore domains, together with biochar–polymer interfacial voids, may contribute to water confinement through adsorption and capillary retention, while the Ca^{2+}-mediated "egg-box" pectin network provides additional physical confinement within the hydrated composite.

Table 3. Water Holding Capacity of Different Pectin Formulations

Formulation	WHC (%)	Indication
Pectin Powder	31.25 ± 2.08^a	Weak WHC; unstable structure.
Pectin Gel	44.11 ± 2.03^b	Gel network enhances WHC and stability.
BPGC	97.90 ± 1.51^c	Very strong, highly stable structure with excellent WHC.

Note: The values (Mean ± SD) in the same row with the same letter show no significant differences at $P \leq 0.05$

Mathematical interpretation of swelling and moisture retention

To evaluate the potential contribution of biochar incorporation to the swelling behavior of BPGC, the experimental results were interpreted using a simplified mass-fraction model, in which the biochar phase was considered a relatively rigid and non-swelling component within the Ca^{2+}-crosslinked pectin network. Under this assumption, incorporation of 10% biochar would reduce the overall swelling capacity because a fraction of the swellable polymer is replaced by a non-swelling solid phase. The theoretical swelling of the composite can therefore be estimated as:

$$S_{theo} = S_{gel}\,(1-w_{bio}) \quad (6)$$

where S_{theo} is the theoretical swelling ratio of BPGC, S_{gel} is the swelling ratio of the calcium-pectin gel, and w_{bio} is the biochar mass fraction. At a biochar loading of 10%, the maximum theoretical swelling ratio calculated from the pectin-gel value of approximately 178% was 160.2%, closely matching the experimentally observed maximum swelling ratio of approximately 160% for BPGC. This agreement suggests that much of the decrease in swelling can be accounted for by the reduced fraction of swellable polymer in the composite under the assumptions of this simplified model. However, changes in network organization and biochar–polymer interfacial interactions may also contribute to the observed swelling behavior (Liu *et al.* 2025).

Importantly, swelling and moisture retention represent different material responses and should not be considered equivalent. Although BPGC exhibited a lower maximum swelling ratio than the pectin gel, the composite retained approximately 60% of its initial retained water after 4 h, compared with approximately 37% for the pectin gel and 11% for pectin. As a simplified reference scenario, assuming that the biochar phase contributes negligibly to moisture retention and that incorporation does not alter the retention behavior of the remaining pectin-gel fraction, the theoretical moisture retention of BPGC was estimated as:

$$MR_{theo} = MR_{gel}\,(1-w_{bio}) \quad (7)$$

where MR_{theo} is the theoretical moisture retention of BPGC and MR_{gel} is the moisture retention of the calcium-pectin gel. At 10% carbon loading, the predicted moisture retention after 4 h was approximately 33.3%, which is substantially lower than the experimentally observed value of approximately 60% for BPGC. This deviation indicates that the moisture-retention behavior cannot be explained solely by replacement of the pectin fraction with non-swelling biochar. Instead, the porous biochar structure and biochar–polymer interfacial spaces may provide additional sites for water confinement, while the Ca^{2+}-crosslinked pectin network may further limit water mobility and moisture loss (Liu *et al.* 2025). Thus, biochar incorporation was associated with reduced swelling while substantially enhancing moisture retention, which may provide an advantageous balance for the intended soil-moisture management application.

Implications for performance under agricultural conditions

Although laboratory experiments using distilled water provide a baseline assessment of the intrinsic hydration and water-retention capacity of BPGC, its performance under realistic agricultural conditions may be influenced by soil salinity, ionic composition, temperature fluctuations, mechanical constraints, and repeated drying–rewetting cycles. In saline environments, elevated concentrations of dissolved ions, particularly Na^{+} and Cl^{-}, can screen electrostatic interactions between charged groups along the pectin chains and reduce the osmotic driving force for swelling relative to distilled water. Conversely, divalent cations such as Ca^{2+} and Mg^{2+} may interact with pectin carboxylate groups and modify the crosslinking density and stability of the characteristic Ca^{2+}-mediated "egg-box" network (Braccini and Pérez 2001; Einhorn-Stoll *et al.* 2016). Consequently, BPGC swelling and water retention under field conditions are expected to depend strongly on the ionic strength and composition of the soil solution.

Soil confinement may also influence composite expansion and pore accessibility. The relatively rigid biochar particles incorporated into the pectin matrix may provide physical reinforcement and restrict excessive polymer-chain expansion. This interpretation is consistent with the present results, in which the maximum observed swelling ratio was lower for BPGC (~160%) than for the Ca^{2+}-crosslinked pectin gel (~178%). Despite its lower swelling capacity, BPGC retained approximately 60% moisture after 4 h, compared with approximately 37% for pectin gel and 11% for pectin, indicating that restricted volumetric swelling does not necessarily compromise moisture retention. The porous biochar structure and biochar–polymer interfacial spaces may contribute to water confinement, while hydrogen bonding and Ca^{2+}-mediated crosslinking can further restrict water mobility within the polymer network (Liu *et al.* 2025).

Temperature fluctuations and successive drying–rewetting events may further affect polymer-chain mobility, water diffusion, crosslink stability, and the physical integrity of BPGC. Biochar particles may potentially improve the dimensional stability of the polymer network during repeated hydration and dehydration; however, these conditions were not directly investigated in the present study. Accordingly, the measured water-holding capacity of 97.9% should be interpreted as performance under the laboratory conditions investigated rather than evidence of long-term cyclic stability. Future studies should therefore evaluate BPGC in representative agricultural soils under different salinity levels, temperatures, mechanical conditions, and repeated drying–rewetting cycles. Long-term pot and field experiments under deficit-irrigation conditions are particularly recommended to establish composite durability, water-release kinetics, effective application rates, irrigation-water savings, and agronomic effectiveness under arid and semi-arid conditions.

Biocompatibility Assessment

Effect of pectin concentration on Bacillus cereus growth

Different concentrations of pectin (1%, 3%, and 6% (w/v)) were evaluated for their effects on the growth of *Bacillus cereus*, a type of soil bacteria that grows under various environmental stress, using optical density (OD) measurements.

As shown in Fig. 9, 1% pectin produced the greatest growth-promoting effect, whereas bacterial growth decreased at the higher pectin concentrations of 3% and 6%. The enhanced growth observed at 1% may be associated with the ability of *Bacillus* spp. to utilize pectin or its degradation products as a carbon source, whereas the reduced growth observed at higher concentrations may reflect concentration-dependent changes in medium properties or substrate accessibility. However, the mechanisms responsible for these differences were not directly investigated in the present study and should therefore be interpreted cautiously.

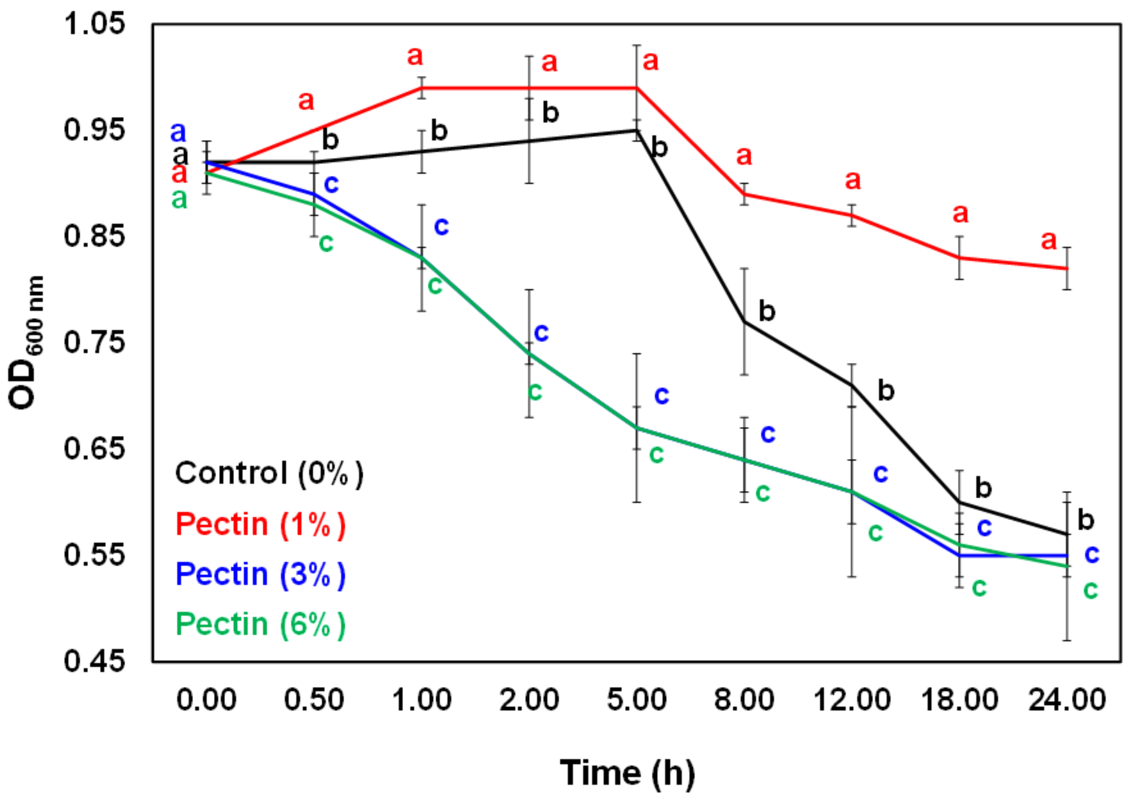

Fig. 9. Growth response of *Bacillus cereus* to various pectin concentrations over 24 h. The values within the same treatment time and letter do not differ significantly at P ≤ 0.05

The growth-promoting response observed at 1% pectin is consistent with the ability of some *Bacillus* strains to utilize pectic substrates and with previous studies showing that pectin concentration influences pectinase production. Prajapati *et al.* (2021) reported high pectinase activity at 1% pectin, while Kottilingal *et al.* (2026) identified an optimum pectin concentration of 5.5 g/L (0.55% w/v) for pectinase production. Overall, the absence of marked growth inhibition at 1% pectin indicates microbial compatibility with the tested bacterial strain under the experimental conditions; however, this finding should not be interpreted as evidence of broader soil-microbial compatibility. Further studies involving beneficial soil microorganisms and more diverse microbial communities are required to establish the ecological effects of the material under realistic soil conditions.

Effect of different pectin formulations on Bacillus cereus growth

The selection of *Bacillus cereus* as a bio-indicator provides a preliminary assessment of the microbial compatibility of BPGC. *B. cereus* is a ubiquitous, Gram-positive, spore-forming bacterium commonly detected in soil and rhizosphere environments, and members of the *Bacillus cereus* group are involved in ecological processes associated with organic matter transformation and nutrient cycling (Saxena *et al.* 2020). In the present study, the absence of detectable growth inhibition in the presence of BPGC indicates that the final composite did not exert appreciable antibacterial effects against the tested organism under the experimental conditions. This observation is consistent with effective post-preparation washing; however, it should not be interpreted as direct confirmation of the complete removal of residual H_3PO_4 or phenolic compounds, which would require specific chemical analyses.

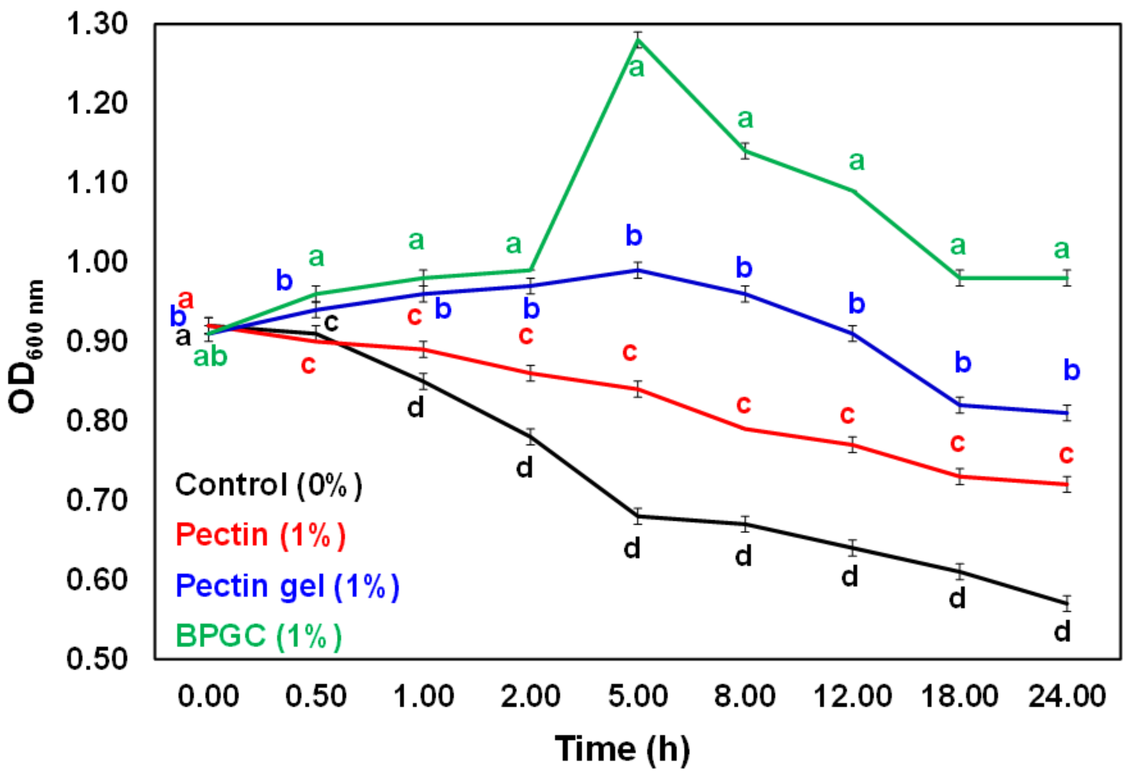

Fig. 10. Growth response of *Bacillus cereus* dependence on pectin, pectin gel, and BPGC (1%) over 24 hours. The values within the same treatment time and letter do not differ significantly at P ≤ 0.05.

The porous structure and moisture-retaining characteristics of carbon-based soil amendments may additionally provide hydrated microsites that support microbial colonization and reduce exposure to desiccation stress, as previously reported for biochar-associated soil microbial habitats (Max *et al.* 2011). Nevertheless, the response of a single bacterial species cannot represent the complexity of indigenous soil microbial communities.

The effects of pectin (1% w/v), pectin gel (1% w/v), and BPGC (1% w/v) on *B. cereus* growth were evaluated over 24 h relative to the control (Fig. 10). Although cell density declined over time across the treatments, BPGC exhibited the highest peak OD_{660} (1.28) and maintained relatively high cell density during the initial 5 h. This response indicates that BPGC was compatible with *B. cereus* growth under the tested conditions. The porous biochar–polymer matrix may provide surfaces favorable for microbial attachment and hydrated microsites, while oxygen-containing functional groups on biochar materials can interact with nutrients and other dissolved species (Hou *et al.* 2022; Kayoumu *et al.* 2025). Pectin gel also supported bacterial growth, reaching a peak OD_{660} of 0.986. Calcium-crosslinked pectin matrices have previously been reported to provide protective microenvironments for bacterial cells under environmental stress (Quan *et al.* 2025).

Seed germination and seedling growth

Tomato (*Solanum lycopersicum*) was selected as the model crop because of its economic importance in arid and semi-arid regions and its sensitivity to water and osmotic stress during early developmental stages. Early seed imbibition, germination, and radicle emergence are particularly dependent on adequate water availability; therefore, tomato provides a suitable biological model for evaluating the phytotoxicity and potential effects of BPGC during early plant establishment. The favorable germination and seedling-growth responses observed with BPGC support its compatibility with early plant development and suggest potential benefits for crop establishment. However, because the present study was restricted to tomato, these findings should not be generalized to other crop species. Future studies should evaluate BPGC using additional drought-sensitive agronomic and horticultural crops, followed by pot and field experiments under controlled water-deficit conditions.

The results in Table 4 illustrated that the application of pectin, pectin gel, and BPGC significantly improved all growth parameters in tomato plantlets (*Solanum lycopersicum* var. cerasiforme) compared to the control. While pectin enhanced shoot and root elongation, the pectin gel presented more declared effect, which may affect water and nutrient uptake due to its physical properties. The BPGC achieved the maximum germination at 98%, with shoot length of 8.31 cm, root length of 4.03 cm, seedling fresh weight (SFW) of 3.27 g, performance index (PI) of 12.34 cm, and seedling vigor index (SVI) of 1209.3 against pectin (1%), pectin gel (1%), and control. The increase in PI (from 8.87 to 12.34 cm) and SVI (from 850.3 to 1209.3) during the treatments confirms that the composite material, which enhances nutrient availability and reduces oxidative stress, also promotes microbial adhesion and strengthens the ability of microorganisms to optimize the seedling rhizosphere environment. Also, Hou *et al.* (2022) found that numerous functional groups on the surface of biochar, including carboxyl, produce a more favorable rhizosphere environment in early plant growth. These results are consistent with the idea that combining organic polymers and adsorbents enhances seed germination by optimizing the rhizosphere environment. Pectin and pectin gels are known to improve soil properties and water retention, thereby enhancing root and shoot growth (Cao and Li 2021).

Evaluating the long-term environmental behavior of soil amendments is essential to ensure their ecological safety and minimize the risk of persistent soil contamination. Compared with non-biodegradable synthetic polymer-based water-retaining materials, the pectin component of BPGC is a naturally derived polysaccharide that is susceptible to microbial and enzymatic degradation in soil, potentially yielding lower-molecular-weight carbohydrates and contributing to soil organic matter. In contrast, the biochar fraction is expected to degrade considerably more slowly and may persist in soil, potentially contributing to long-term carbon storage in soil and influencing soil physicochemical properties (Gross *et al.* 2024). The contrasting degradation rates of these two components therefore suggest a gradual transition from a polymer-supported composite toward a more persistent biochar fraction.

Table 4. Effects of Pectin, Pectin Gel, and BPGC on Germination, Shoot Length, Root Length, SFW, PI, and SVI in Tomato Plantlets

Treatment	Control (0%)	Pectin (1%)	Pectin Gel (1%)	BPGC (1%)
Germination (%)	96.0 ± 1.0^{ab}	96.0 ± 1.0^{ab}	97.0 ± 1.0^{ab}	98.0 ± 1.0^{a}
Shoot length (cm)	6.15 ± 0.99^{c}	7.18 ± 1.27^{b}	7.31 ± 1.05^{b}	8.31 ± 1.00^{a}
Root length (cm)	2.72 ± 0.10^{d}	3.12 ± 0.11^{c}	3.51 ± 0.10^{b}	4.03 ± 0.10^{a}
SFW (g)	2.31 ± 0.12^{c}	2.54 ± 0.11^{c}	2.94 ± 0.16^{b}	3.27 ± 0.20^{a}
PI (cm)	8.87 ± 0.92^{d}	10.30 ± 1.35^{c}	10.82 ± 0.97^{b}	12.34 ± 1.20^{a}
SVI	850.3 ± 80.0^{c}	988.5 ± 79.3^{b}	1049.6 ± 86.3^{b}	1209.3 ± 129.5^{a}

Values (Mean ± SD) in same row with same letter show no significant differences at $P \leq 0.05$.

Phytotoxicity and enzymatic Activity

The results in Table 5 indicated that the tested formulations did not suppress the measured enzymatic activities relative to the control. The BPGC significantly improved protease (186 U/g FW) and lipase (201 U/g FW) activities compared with the control (157 U/g FW) and (118 U/g FW), respectively, suggesting enhanced hydrolytic enzyme activity associated with reserve mobilization during early seedling development. Together with the germination and growth results, these responses provide no indication of phytotoxic effects of BPGC under the tested conditions. This performance may attributed to the highly biocompatible pectin gel matrix, which preserves a hydrated microenvironment in the soil (Gawkowska *et al.* 2018), and to the high adsorptive capacity of biochar, which removes allelopathic inhibitors (Bao *et al.* 2024). While α-amylase activity showed noticeable increases (up to 0.603 mg maltose/g FW), the lack of significant differences among treatments indicates that the formulations did not significantly alter α-amylase activity under the tested conditions (Muralikrishna and Nirmala 2005).

Table 5. Effects of Pectin, Pectin Gel, and BPGC on Protease, Lipase, and α-Amylase Activities in Tomato Plantlets

Parameter	Control (0%)	Pectin (1%)	Pectin Gel (1%)	BPGC (1%)
Protease Activity (U/g FW)	157.33 ± 9.45[b]	160.00 ± 13.23[b]	180.67 ± 5.51[ab]	185.67 ± 11.06[a]
Lipase Activity (U/g FW)	117.67 ± 2.52[d]	161.00 ± 3.00[c]	177.67 ± 3.21[b]	201.00 ± 9.17[a]
α-Amylase Activity (mg maltose/g FW)	0.487 ± 0.025[a]	0.493 ± 0.085[a]	0.587 ± 0.047[a]	0.603 ± 0.070[a]

Values (Mean ± SD) in same row with the same letter show no significant differences at $P \leq 0.05$.

Sustainability and Techno-Economic Considerations

Environmental sustainability considerations

To substantiate the circular bioeconomy potential of the proposed valorization pathway, the environmental trade-offs associated with H_3PO_4-assisted biochar production should be critically considered alongside its resource-recovery benefits. The thermal treatment applied in this study at 350 °C represents a relatively low-temperature regime compared with conventional physical activation using steam or CO_2, which commonly requires substantially higher temperatures, and may therefore reduce the thermal energy requirements of the carbonization step (Ahmad *et al.* 2021). Moreover, H_3PO_4 acts as a dehydrating agent during biomass conversion, promoting structural development and limiting tar formation at relatively low carbonization temperatures, which may favor carbon yield and reduce the severity of thermal processing (Abdel daiem *et al.* 2019).

Nevertheless, H_3PO_4-assisted treatment introduces environmental burdens associated with phosphoric acid production and consumption, as well as water requirements and wastewater generation during post-carbonization washing. In the present study, the carbonized material was washed with distilled water until the filtrate reached approximately pH 6. At an industrial scale, acid and phosphorus recovery or recycling strategies could potentially reduce reagent consumption and phosphate-containing wastewater generation; recent studies have demonstrated the feasibility of recovering and reusing phosphorus species from H_3PO_4- treatment washing streams in subsequent biomass treatment cycles, thereby reducing chemical consumption and associated environmental impacts (Fan *et al.* 2026). H_3PO_4 treatment can promote pore development and surface functionalization of lignocellulosic precursors, including olive pomace; however, appropriate chemical recovery and wastewater-management strategies should be implemented to improve the environmental sustainability of the process (Alrowais *et al.* 2026; Fan *et al.* 2026).

From an agricultural perspective, H_3PO_4 treatment may also introduce phosphorus-containing surface species with potential agronomic value (Zhao *et al.* 2025). Phosphorus retained on carbonaceous materials may potentially contribute to gradual nutrient release and reduced phosphorus mobility, as reported for phosphorus-enriched biochar and related soil amendments (Song *et al.* 2025). This potential agronomic co-benefit warrants further investigation.

Overall, converting phenolic-rich olive pomace into a functional water-retaining composite provides a promising pathway for recovering value from an agro-industrial residue that otherwise requires appropriate management or disposal (Puglia *et al.* 2021). However, the environmental benefits of the complete BPGC production pathway cannot be conclusively established from the present experiments alone because a comprehensive life-cycle assessment was not performed. Future studies should therefore quantify energy consumption, greenhouse-gas emissions, water demand, chemical recovery efficiency, wastewater-treatment requirements, biochar yield, transportation impacts, and end-of-life behavior through a comprehensive life-cycle assessment with a clearly defined system boundary and functional unit. Such analysis would provide a more rigorous basis for evaluating the overall environmental sustainability and circular-bioeconomy performance of BPGC at larger production scales.

Economic and processing considerations

A critical challenge in scaling carbonaceous soil amendments is balancing material performance, production yield, and processing costs. Conventional physical and high-temperature chemical activation generally requires greater thermal energy and can increase carbon burn-off, potentially reducing material yield and increasing production costs (Arfasa and Tilahun 2025). Compared with conventional high-temperature activated carbon production, the low-temperature H_3PO_4-assisted biochar production route used in the present study may reduce thermal energy requirements and preserve a greater fraction of the carbonaceous material, although chemical consumption, washing requirements, and reagent recovery must also be considered when evaluating overall production costs (Arfasa and Tilahun 2025; Fan *et al.* 2026). Conventional untreated biochar generally requires less intensive processing; however, additional chemical treatment can modify pore development and surface functionality for specific applications (Arfasa and Tilahun 2025).

The H_3PO_4-assisted treatment at 350 °C used in the present study therefore represents a relatively mild biochar-production approach. The resulting biochar material exhibited oxygen-containing surface functionalities and predominantly mesoporous characteristics, including a DFT pore domain at 2.94 nm. These characteristics may facilitate integration of the carbon phase within the pectin matrix and contribute to capillary water retention (Alrowais *et al*. 2026), while the relatively low treatment temperature limits the thermal requirements associated with conventional high-temperature activation (Arfasa and Tilahun 2025). Nevertheless, the economic and environmental advantages of this approach should be confirmed through detailed biochar mass-yield, energy-consumption, chemical-recovery, and cost analyses at larger production scales (Fan *et al.* 2026).

Preliminary techno-economic assessment

The preliminary TEA indicated that the valorization of olive pomace into BPGC may offer favorable economic potential under the technical and market assumptions adopted in this study. At the assumed production capacity of 200 t/year, the estimated BPGC production cost was approximately $1.60/kg, compared with an assumed selling price of $3.00/kg, corresponding to a gross margin of approximately $1.40/kg (46.7%). Annual revenue was estimated at approximately $600,000, while the corresponding annual production cost was approximately $320,000, resulting in an estimated annual operating cash flow of approximately $280,000. The use of low-cost olive pomace, valued at approximately $20/t, contributes to the potential economic attractiveness of converting this agro-industrial residue into a value-added water-retaining soil amendment. Such valorization is consistent with circular-bioeconomy strategies aimed at recovering economic value from agricultural residues while reducing their associated management burden (Staffas *et al.* 2013; Sharma *et al.* 2020; Ubando *et al.* 2020).

Based on an estimated initial capital expenditure of approximately $0.90 million, a project lifetime of 10 years, and a discount rate of 10%, and assuming a constant annual operating cash flow over the project lifetime, the process yielded an estimated NPV of approximately $0.82 million, an IRR of approximately 28.6%, and a simple payback period of approximately 3.2 years (Table 6). The positive NPV indicates that the projected discounted cash flows exceed the estimated initial investment under the adopted assumptions, while the IRR and payback period indicate potential economic viability within the evaluated scenario. Nevertheless, these indicators should be interpreted as preliminary scenario-based estimates rather than evidence of commercial profitability, because actual economic performance will depend on production scale, reagent and energy costs, capital requirements, process efficiency, and market price. Sensitivity analysis and pilot-scale validation are therefore needed to evaluate the robustness of these preliminary economic estimates.

Table 6. Preliminary Techno-economic Indicators of BPGC Production

Economic Indicator	Value
Production capacity	200 t/year
Operating period	300 days/year
Approximate daily production	667 kg/day
Project lifetime	10 years
Discount rate	10%
Olive pomace feedstock cost	$20/t
BPGC production cost	≈ $1.60/kg
Assumed selling price	$3.00/kg
Gross margin	≈ $1.40/kg (46.7%)
Estimated initial CAPEX	≈ $0.90 million
Estimated annual revenue	≈ $600,000/year
Estimated annual production cost	≈ $320,000/year
Estimated annual operating cash flow	≈ $280,000/year
NPV at 10%	≈ $0.82 million
IRR	≈ 28.6%
Simple payback period	≈ 3.2 years

To further assess the practical and economic relevance of BPGC, its performance was compared with representative conventional and bio-based soil moisture-retention materials (Table 7). Compared with conventional synthetic superabsorbent polymers (SAPs), BPGC provides a bio-based approach to soil moisture management by integration of olive pomace-derived pectin and biochar. While synthetic SAPs are established water-retention materials, bio-based hydrogels and carbon–polymer composites are increasingly being investigated as renewable alternatives (Muhammad *et al.* 2025; Said *et al.* 2023; Kanagalakshmi *et al.* 2024; Liu *et al.* 2025; Shu *et al.* 2025). In the present study, BPGC achieved a water-holding capacity of 97.9% and retained 60% moisture after 4 h, while its estimated production cost was approximately $1.60/kg under the adopted techno-economic assumptions. Together, these findings demonstrate the potential for converting low-cost olive pomace into a functional water-retaining soil amendment.

Limitations and Future Work

The present study was conducted under controlled laboratory conditions; therefore, long-term performance under realistic soil conditions, the effects of salinity and repeated drying–rewetting cycles, phosphorus release and bioavailability, and long-term composite stability were not evaluated. Biological testing was limited to tomato and a single bacterial species. A comprehensive life-cycle assessment and pilot-scale techno-economic validation were also beyond the scope of the present study. Future studies should include larger replicate numbers to strengthen statistical robustness, optimize biochar preparation and BPGC production conditions, evaluate phosphorus availability and environmental impacts, assess additional drought-sensitive crop species relevant to arid regions, and conduct long-term pot and field trials under different soil and irrigation conditions. Complementary analyses are needed, including X-ray diffraction, thermogravimetric analysis, and surface-chemical characterization, to further validate the composite structure and interactions. Evaluation of beneficial soil microorganisms and more diverse microbial communities is also recommended to better assess the ecological effects of BPGC under realistic agricultural conditions.

Table 7. Practical Comparison of BPGC with Representative Soil Moisture-Retention Materials

Material	Source/Type	Water-Retention Characteristics	Practical/Economic Consideration	Main Limitation	Reference
SAPs	Synthetic hydrophilic polymers	High water absorption and retention; widely applied for agricultural water management	Commercially established; performance depends on formulation and application conditions	Synthetic origin and environmental sustainability considerations	Muhammad *et al.* 2025
Bio-based hydrogels	Natural polymers	High water affinity through swelling, hydrogen bonding, and polymer-network water immobilization	Renewable alternative to synthetic SAPs	Performance and durability depend on polymer composition and network structure	Said *et al.* 2023; Liu *et al.* 2025
Pectin–carbon hydrogel	Pectin + carbonaceous material	Enhanced hydrophilicity and water-holding characteristics	Combines renewable polymer with porous carbon functionality	Scale-up and long-term field performance require validation	Kanagalakshmi *et al.* 2024
Biopolymer-modified biochar	Biomass-derived carbon + biopolymer	Improved water absorption and retention through porous and hydrophilic domains	Utilizes biomass-derived materials	Performance depends on biochar properties, modification, and soil conditions	Shu *et al.* 2025
BPGC (present study)	**Olive pomace-derived pectin + biochar**	**WHC 97.9%; 60% moisture retention after 4 h**	**Valorizes low-cost olive pomace; estimated production cost of ≈ $1.60/kg under the adopted techno-economic assumptions**	**Field application rate, service life, scale-up economics, and long-term performance require further validation**	**Present study**

CONCLUSIONS

This study demonstrated the effective valorization of olive pomace into functional materials, namely pectin, pectin gel, and biochar-pectin gel composite (BPGC), for sustainable agricultural applications.

1. The H_3PO_4-treated olive pomace biochar exhibited predominantly mesoporous characteristics, while scanning electron microscopy (SEM) and Fourier transform infrared (FTIR) analyses confirmed its successful physical integration within the Ca^{2+}-crosslinked pectin matrix, supporting the successful formation of BPGC.
2. Swelling and water retention studies revealed that pectin achieved rapid swelling (121% within 10 min, reaching ~195% within 2 h), whereas BPGC showed superior moisture retention (60.0%) and water-holding capacity (97.9%), outperforming the individual pectin-based formulations.
3. Biological assessments showed no detectable phytotoxic effects, with high germination rates (96%–98%) across all treatments. BPGC significantly enhanced plant growth parameters, including shoot length (8.31 cm), root length (4.03 cm), and seed vigor index (1210). Enzymatic activities were also improved, with protease and lipase reaching 186 and 201 U/g FW, respectively.
4. Overall, BPGC represents a promising bio-based water-retaining soil amendment, showing microbial compatibility, no detectable phytotoxicity, and high water-retention performance under the tested conditions. These findings support its potential for soil-moisture management in arid and semi-arid agricultural systems.

ACKNOWLEDGMENTS

This work was funded by the Deanship of Graduate Studies and Scientific Research at Jouf University under grant No. (DGSSR-2025-02-01311).

During the preparation of this manuscript, the authors used ChatGPT (OpenAI) to assist with language editing and improving the clarity and organization of the text. The authors reviewed and edited the content and take full responsibility for the scientific accuracy and integrity of the work.

REFERENCES CITED

Abdel Daiem, M., Alotaibi, A., Alosime, E., Zaidi, B., and Said, N. (2020). "Structural-property relationship in activated carbon synthesized from rice straw for electronic application," *Polish Journal of Environmental Studies* 29(5), 3535-3547. https://doi.org/10.15244/pjoes/117761

Abdel Daiem, M. M., Rashad, A. M., Said, N., and Abdel-Gawwad, H. A. (2021). "An initial study about the effect of activated carbon nano-sheets from residual biomass of olive trees pellets on the properties of alkali-activated slag pastes," *Journal of Building Engineering* 44, article 102661. https://doi.org/10.1016/j.jobe.2021.102661

Abdel Daiem, M. M., Sánchez-Polo, M., Rashed, A. S., Kamal, N., and Said, N. (2019). "Adsorption mechanism and modelling of hydrocarbon contaminants onto rice straw

activated carbons," *Polish Journal of Chemical Technology* 21(4), 1-12. https://doi.org/10.2478/pjct-2019-0032
Abdelfattah, A., and Mostafa, H. (2024). "Potential of soil conditioners to mitigate deficit irrigation impacts on agricultural crops: A review," *Water Resources Management* 38(8), 2961-2976. https://doi.org/10.1007/s11269-024-03800-4
Adamczak, M. I., Martinsen, Ø. G., Smistad, G., and Hiorth, M. (2016). "Water sorption properties of HM-pectin and liposomes intended to alleviate dry mouth," *International Journal of Pharmaceutics* 506(1), 201-206. https://doi.org/10.1016/j.ijpharm.2016.04.050
Adetunji, L. R., Adekunle, A., Orsat, V., and Raghavan, V. (2017). "Advances in the pectin production process using novel extraction techniques: A review," *Food Hydrocolloids* 62, 239-250. https://doi.org/10.1016/j.foodhyd.2016.08.015
Agbna, G. H. D., and Zaidi, S. J. (2025). "Hydrogel performance in boosting plant resilience to water stress—A review," *Gels* 11(4), article 276. https://doi.org/10.3390/gels11040276
Ahmad, A. A., Al-Raggad, M., and Shareef, N. (2021). "Production of activated carbon derived from agricultural by-products via microwave-induced chemical activation: a review," *Carbon Letters* 31(5), 957-971. https://doi.org/10.1007/s42823-020-00208-z
Ali, A., Jabeen, N., Chachar, Z., Chachar, S., Ahmed, S., Ahmed, N., Laghari, A. A., Sahito, Z. A., Farruhbek, R., and Yang, Z. (2025). "The role of biochar in enhancing soil health & interactions with rhizosphere properties and enzyme activities in organic fertilizer substitution," *Frontiers in Plant Science* 16, article 1595208. https://doi.org/10.3389/fpls.2025.1595208
Alimenti, C., Lianza, M., Antognoni, F., Giusti, L., Bistoni, O., Liotta, L., Angeloni, C., Lupidi, G., and Beghelli, D. (2023). "Characterization and biological activities of in vitro digested olive pomace polyphenols evaluated on ex vivo human immune blood cells," *Molecules* 28(5), article 2122. https://doi.org/10.3390/molecules28052122
Alouiz, I., Benhadj, M., Harboul, K., Boukhris, M., Elmontassir, D., Sennoune, M., Amarouch, M. Y., and Mazouzi, D. (2025). "Activated carbon from olive pomace for hexavalent chromium removal: synthesis, characterization, and adsorption mechanism analysis," *Scientific Reports* 15(1), article 18576. https://doi.org/10.1038/s41598-025-95278-2
Alrowais, R., Abdel Daiem, M. M., Yousef, R., Ahmed, O., Metwally, A. A., and Said, N. (2026). "Techno-economic and sustainability assessment of a circular two-stage olive mill wastewater treatment system using olive pomace-derived activated carbon," *BioResources* 21(2), 4977-5009. https://doi.org/10.15376/biores.21.2.4977-5009
Arfasa, G. F., and Tilahun, Z. A. (2025). "Life-cycle impacts of biochar, MOFs, and biomass adsorbents: A meta-analysis for wastewater and carbon management," *Environmental Challenges* 2025, article 101331. https://doi.org/10.1016/j.envc.2025.101331
Asare, F., Gazo, R., Mo, J., Haviarova, E., Quesada, H. J., Rahmani, S. R., Owusu, F. W., Saraugi, S. S., and Routray, W. (2026). "Techno-economic analysis of farmer-scale biochar production from agricultural residues in the U.S. Corn Belt: A comparison of three low-cost kiln architectures," *Bioresource Technology* 2026, article 135686. https://doi.org/10.1016/j.biortech.2026.135686
Bao, L., Zhao, X., Kang, G., Suzuki, K., Ismail, T., Fujii, Y., and Motoki, S. (2024). "Assessment of the allelopathic activity of various parts of platycodon (*Platycodon*

grandiflorus) and its mitigation by activated carbon," *Agronomy* 14(2), article 385. https://doi.org/10.3390/agronomy14020385

Bashan, Y., and de-Bashan, L. E. (2010). "How the plant growth-promoting bacterium *Azospirillum* promotes plant growth—a critical assessment," *Advances in Agronomy* 108, 77-136. https://doi.org/10.1016/S0065-2113(10)08002-8

Bermúdez-Oria, A., Rodríguez-Juan, E., Rodríguez-Gutiérrez, G., Fernández-Prior, Á., and Fernández-Bolaños, J. (2021). "Effect of the olive oil extraction process on the formation of complex pectin–polyphenols and their antioxidant and antiproliferative activities," *Antioxidants* 10(12), article 1858. https://doi.org/10.3390/antiox10121858

Braccini, I., and Pérez, S. (2001). "Molecular basis of Ca^{2+}-induced gelation in alginates and pectins: The egg-box model revisited," *Biomacromolecules* 2(4), 1089-1096. https://doi.org/10.1021/bm010008g

Cao, L., and Li, N. (2021). "Activated-carbon-filled agarose hydrogel as a natural medium for seed germination and seedling growth," *International Journal of Biological Macromolecules* 177, 383-391. https://doi.org/10.1016/j.ijbiomac.2021.02.097

Černá, M., Barros, A. S., Nunes, A., Rocha, S. M., Delgadillo, I., Čopíková, J., and Coimbra, M. A. (2003). "Use of FT-IR spectroscopy as a tool for the analysis of polysaccharide food additives," *Carbohydrate Polymers* 51(4), 383-389. https://doi.org/10.1016/S0144-8617(02)00259-X

Ciriminna, R., Fidalgo, A., Delisi, R., Ilharco, L. M., and Pagliaro, M. (2016). "Pectin production and global market," *Agro Food Industry Hi-Tech* 27(5), 17-20.

Chafi, S., Cuevas-Aranda, M., Martínez-Cartas, M. L., and Sánchez, S. (2025). "Production of bioadsorbents via low-temperature pyrolysis of exhausted olive pomace for the removal of methylene blue from aqueous media," *Molecules* 30(15), article 3254. https://doi.org/10.3390/molecules30153254

Correa-Quiroz, J. J., Toribio-barrueto, M. A., and Castro-Vargas, C. (2025). "IoT system with ESP32 for smart drip irrigation and climate monitoring in greenhouses," *Emerging Science Journal* 9(3), 1133-1157. https://doi.org/10.28991/ESJ-2025-09-03-01

Das, S. K., and Ghosh, G. K. (2022). "Hydrogel-biochar composite for agricultural applications and controlled release fertilizer: a step towards pollution free environment," *Energy* 242, article 122977. https://doi.org/10.1016/j.energy.2021.122977

Deniz, F., Başgöz, Ö., Güler, Ö., and Mazmancı, M. A. (2022). "Characterization and dye adsorption effectiveness of activated carbon synthesized from olive pomace," *Environmental Research and Technology* 5(4), 369-379. https://doi.org/10.35208/ert.1163939

Dranca, F., and Oroian, M. (2018). "Extraction, purification and characterization of pectin from alternative sources with potential technological applications," *Food Research International* 113, 327-350. https://doi.org/10.1016/j.foodres.2018.06.065

Einhorn-Stoll, U., Vasileva, E., Hecht, T., and Drusch, S. (2016). "Investigation of pectin-water interactions: A practical approach," in: *Gums and Stabilisers for the Food Industry 18: Hydrocolloid Functionality for Affordable and Sustainable Global Food Solutions*, The Royal Society of Chemistry, 1–12.

El-Shatoury, S., El-Baz, A., Abdel Daiem, M., and El-Monayeri, D. (2014). "Enhancing wastewater treatment by commercial and native microbial inocula with factorial design," *Life Science Journal* 11(7), article marslsj110714.108.

https://doi.org/10.7537/marslsj110714.108
Enaime, G., Dababat, S., Wichern, M., and Lübken, M. (2024). “Olive mill wastes: From wastes to resources,” *Environmental Science and Pollution Research* 31(14), 20853-20880. https://doi.org/10.1007/s11356-024-32468-x
Fan, M., Qi, M., Liu, Y., Meng, X., Jiang, Y., Li, B., Liu, W., Zhang, S., Wang, Y., and Hu, X. (2026). “Closing the loop to minimize the generation of liquid waste: Recycling phosphorus species from solid residue to activate with H_3PO_4 for next-round activating biomass,” *Green Chemistry* 28(24), 10168-10186. https://doi.org/10.1039/d5gc06796k
FAO. (2021). "The state of the world’s land and water resources for food and agriculture (SOLAW) – Managing systems at risk," *Food and Agriculture Organization of the United Nations*.
Farrukh, S., Fan, X., Karim, S. S., Yu, Z., and Lu, G. (2025). “Synergistic effects of structured and powdered Calcium chloride-activated carbon composites on ammonia adsorption: The role of salt distribution and pH-controlled crosslinking,” *Emergent Materials* 8(6), 5217-5240. https://doi.org/10.1007/s42247-025-01106-8
Freitas, C. M. P., Coimbra, J. S. R., Souza, V. G. L., and Sousa, R. C. S. (2021). “Structure and applications of pectin in food, biomedical, and pharmaceutical industry: A review,” *Coatings* 11(8), article 922. https://doi.org/10.3390/coatings11080922
Fuentes-Alventosa, J. M., Rodríguez-Gutiérrez, G., Jaramillo-Carmona, S., Espejo-Calvo, J. A., Rodríguez-Arcos, R., Fernández-Bolaños, J., Guillén-Bejarano, R., and Jiménez-Araujo, A. (2009). “Effect of extraction method on chemical composition and functional characteristics of high dietary fibre powders obtained from asparagus by-products,” *Food Chemistry* 113(2), 665-671. https://doi.org/10.1016/j.foodchem.2008.07.075
Gawkowska, D., Cybulska, J., and Zdunek, A. (2018). “Structure-related gelling of pectins and linking with other natural compounds: A review,” *Polymers* 10(7), article 762. https://doi.org/10.3390/polym10070762
Gross, A., Bromm, T., Polifka, S., Fischer, D., and Glaser, B. (2024). “Long-term biochar and soil organic carbon stability – Evidence from field experiments in Germany,” *Science of The Total Environment* 954, article 176340. https://doi.org/10.1016/j.scitotenv.2024.176340
Gómez-Cruz, I., del Mar Contreras, M., Romero, I., and Castro, E. (2024). “Towards the integral valorization of olive pomace-derived biomasses through biorefinery strategies,” *ChemBioEng Reviews* 11(2), 253-277. https://doi.org/10.1002/cben.202300045
Guerboub, L., Soufi-Maddi, O., Ouldsaadi, L., Medouni-Haroune, L., Bachir-bey, M., Madani, K., and Boulekbache-Makhlouf, L. (2025). “Characterization of chemlal olive pomace and its extracted oil: Chemical composition, quality indices, and FTIR analysis,” *Journal of Food Measurement and Characterization* 19(12), 9400-9411. https://doi.org/10.1007/s11694-025-03620-z
Horwitz, W., and Latimer, G. W. (2006). *The Methods of the Association of Official Agricultural Chemists*, AOAC, 19.
Hosseini, S. S., Khodaiyan, F., and Yarmand, M. S. (2016). “Aqueous extraction of pectin from sour orange peel and its preliminary physicochemical properties,” *International Journal of Biological Macromolecules* 82, 920-926. https://doi.org/10.1016/j.ijbiomac.2015.11.007

Hou, J., Yu, J., Li, W., He, X., and Li, X. (2022). "The effects of chemical oxidation and high-temperature reduction on surface functional groups and the adsorption performance of biochar for sulfamethoxazole adsorption," *Agronomy* 2022, article 12020510. https://doi.org/10.3390/agronomy12020510

Ibeh, P. O., García-Mateos, F. J., Rosas, J. M., Rodríguez-Mirasol, J., and Cordero, T. (2019). "Activated carbon monoliths from lignocellulosic biomass waste for electrochemical applications," *Journal of the Taiwan Institute of Chemical Engineers* 97, 480-488. https://doi.org/10.1016/j.jtice.2019.02.019

ISTA. (2020). *Seed Germination Testing Protocols*.

Kabiri, K., Omidian, H., Zohuriaan-Mehr, M. J., and Doroudiani, S. (2011). "Superabsorbent hydrogel composites and nanocomposites: A review," *Polymer Composites* 32(2), 277-289. https://doi.org/10.1002/pc.21046

Kačuráková, M., Capek, P., Sasinková, V., Wellner, N., and Ebringerová, A. (2000). "FT-IR study of plant cell wall model compounds: Pectic polysaccharides and hemicelluloses," *Carbohydrate Polymers* 43(2), 195-203. https://doi.org/10.1016/S0144-8617(00)00151-X

Kanagalakshmi, M., Devi, S. G., Subasini, S., Amalan, A. J., and Pius, A. (2024). "Experimental assessment of biostimulants on mung bean growth on a soilless culture system using superabsorbent pectin based hydrogel," *International Journal of Biological Macromolecules* 273, article 133058. https://doi.org/10.1016/j.ijbiomac.2024.133058

Kayoumu, M., Wang, H., and Duan, G. (2025). "Interactions between microbial extracellular polymeric substances and biochar, and their potential applications: A review," *Biochar* 7(1), 62. https://doi.org/10.1007/s42773-025-00452-4

Khoder, M., Tsapis, N., Huguet, H., Besnard, M., Gueutin, C., and Fattal, E. (2009). "Removal of ciprofloxacin in simulated digestive media by activated charcoal entrapped within zinc-pectinate beads," *International Journal of Pharmaceutics* 379(2), 251-259. https://doi.org/10.1016/j.ijpharm.2009.05.035

Kottilingal, L. S., Paramasivam, S., Sivaprakasam, S., Meera, C. R., and Chinnaiyan, U. (2026). "Optimization of pectinase production from *Bacillus velezensis* isolated from agro-waste using response surface methodology," *Journal of Pure and Applied Microbiology* 20, 459-469. https://doi.org/10.22207/JPAM.20.1.33

Kyomugasho, C., Christiaens, S., Van de Walle, D., Van Loey, A. M., Dewettinck, K., and Hendrickx, M. E. (2016). "Evaluation of cation-facilitated pectin-gel properties: Cryo-SEM visualisation and rheological properties," *Food Hydrocolloids* 61, 172-182. https://doi.org/10.1016/j.foodhyd.2016.05.018

Lamanna, M., Convertini, S., Puglisi, R., Losacco, D., Bari, G., Tarasco, E., and Roma, R. (2026). "Environmental and economic sustainability assessment of biological treatment options for organic wastes and agro-industrial by-products: A scoping review," *Sustainability* 18(6), article 3095. https://doi.org/10.3390/su18063095

Liu, Y., Shen, S., Duan, Z., Deng, J., and Fan, D. (2025). "Hydrogels for long-term moisture retention under ambient conditions: Inhibiting the evaporation of free water from macroscopic to molecular scales," *Advanced Functional Materials* 35(47), article 2504356. https://doi.org/10.1002/adfm.202504356

Manrique, G. D., and Lajolo, F. M. (2002). "FT-IR spectroscopy as a tool for measuring degree of methyl esterification in pectins isolated from ripening papaya fruit," *Postharvest Biology and Technology* 25(1), 99-107. https://doi.org/10.1016/S0925-5214(01)00160-0

Mata, Y. N., Blázquez, M. L., Ballester, A., González, F., and Muñoz, J. A. (2009). "Sugar-beet pulp pectin gels as biosorbent for heavy metals: preparation and determination of biosorption and desorption characteristics," *Chemical Engineering Journal* 150(2–3), 289-301. https://doi.org/10.1016/j.cej.2009.01.001

Max, K., Yael, M. H., Zohar, P., R., G. E., Yigal, E., and Eddie, C. (2011). "Impact of Biochar application to soil on the root-associated bacterial community structure of fully developed greenhouse pepper plants," *Applied and Environmental Microbiology* 77(14), 4924-4930. https://doi.org/10.1128/AEM.00148-11

Millán-Linares, M. C., Montserrat-de la Paz, S., and Martin, M. E. (2021). "Pectins and olive pectins: From biotechnology to human health," *Biology* 10(9), article 860. https://doi.org/10.3390/biology10090860

Morán-Alarcón, L. C., Galán-Martín, Á., del Mar Contreras, M., and Castro, E. (2026). "Recent advances and future perspectives in the valorization of olive biomass for sustainable biorefinery applications," *Renewable and Sustainable Energy Reviews*, 226, article 116438. https://doi.org/10.1016/j.rser.2025.116438

Morim, A. C., Madaleno, M., Tarelho, L. A. C., and Silva, F. C. (2025). "Financial feasibility of biochar production: A comparative analysis of business scenarios," *Journal of Cleaner Production* 536, article 147167. https://doi.org/10.1016/j.jclepro.2025.147167

Muhammad, M., Tawfic, M. L., Taha, M., and Elsabbagh, A. (2025). "Design and manufacturing of superabsorbent polymers (SAPs) for agriculture in arid areas," *Scientific Reports* 15(1), article 16186. https://doi.org/10.1038/s41598-025-99666-6

Muñoz-Almagro, N., Valadez-Carmona, L., Mendiola, J. A., Ibáñez, E., and Villamiel, M. (2019). "Structural characterisation of pectin obtained from cacao pod husk. Comparison of conventional and subcritical water extraction," *Carbohydrate Polymers* 217, 69-78. https://doi.org/10.1016/j.carbpol.2019.04.040

Muralikrishna, G., and Nirmala, M. (2005). "Cereal α-amylases—an overview," *Carbohydrate Polymers* 60(2), 163-173. https://doi.org/10.1016/j.carbpol.2004.12.002

Neha, K., Anitha, R., Subashini, R., Natarajan, A., and Sridhar, T. M. (2019). "Synthesis and characterization of chitosan/potato peel powder-based hydrogel and its in vitro antimicrobial activity," *Journal of Applied Pharmaceutical Science* 9(9), 66-71. https://doi.org/10.7324/JAPS.2019.90909

Pattarapisitporn, A., and Noma, S. (2025). "Alternative solvents for pectin extraction: Effects of extraction agents on pectin structural characteristics and functional properties," *Foods* 14(15), article 2644. https://doi.org/10.3390/foods14152644

Parascanu, M. M., Puig Gamero, M., Sánchez, P., Soreanu, G., Valverde, J. L., and Sanchez-Silva, L. (2018). "Life cycle assessment of olive pomace valorisation through pyrolysis," *Renewable Energy* 122, 589-601. https://doi.org/https://doi.org/10.1016/j.renene.2018.02.027

Pérez-baca, M. S., Sambrano-luna, K. L., Sánchez-ramírez, J. M., Cabana-cáceres, M., Castro-vargas, C., and Castro-Vargas, C. (2024). "Design and implementation of an automated irrigation control for home plantations," *Indonesian Journal of Electrical Engineering and Computer Science* 35(3), 1437-1446. https://doi.org/10.11591/ijeecs.v35.i3.pp1437-1446

Puglia, D., Pezzolla, D., Gigliotti, G., Torre, L., Bartucca, M. L., and Del Buono, D. (2021). "The opportunity of valorizing agricultural waste, through its conversion into biostimulants, biofertilizers, and biopolymers," *Sustainability* 13(5), article 2710.

https://doi.org/10.3390/su13052710
Prado-Acebo, I., Cubero-Cardoso, J., Lu-Chau, T. A., and Eibes, G. (2024). "Integral multi-valorization of agro-industrial wastes: A review," *Waste Management* 183, 42-52. https://doi.org/10.1016/j.wasman.2024.05.001
Prajapati, J., Dudhagara, P., and Patel, K. (2021). "Production of thermal and acid-stable pectinase from Bacillus subtilis strain BK-3: Optimization, characterization, and application for fruit juice clarification," *Biocatalysis and Agricultural Biotechnology* 35, article 102063. https://doi.org/10.1016/j.bcab.2021.102063
Prasertsit, K., Rattanapong, W., and Tongurai, C. (2021). "Effect of fatty acid methyl ester on the mass transfer and rate of an acid transesterification reaction," *Reaction Kinetics, Mechanisms and Catalysis* 133(2), 971-981. https://doi.org/10.1007/s11144-021-02031-7
Quan, Y., Shao, H., Wang, N., Gao, Z., and Jin, M. (2025). "Microenvironment-sensitive hydrogels as promising drug delivery systems for co-encapsulating microbial homeostasis probiotics and anti-inflammatory drugs to treat periodontitis," *Materials Today Bio* 32, article 101711. https://doi.org/10.1016/j.mtbio.2025.101711
Raihani, Z., Chikri, R., Talbi, S., Elhadiri, N., and Rabi, S. (2025). "Performance of olive pomace as an alternative adsorbent pharmaceutical contaminant removal from water. A review," *International Journal of Environmental Analytical Chemistry* 105(16), 4405-4431. https://doi.org/10.1080/03067319.2024.2368265
Rani, P., Bansal, M., and Pathak, V. V. (2022). "Experimental and kinetic studies for improvement of biogas production from KOH pretreated wheat straw," *Current Research in Green and Sustainable Chemistry* 5, article 100283. https://doi.org/10.1016/j.crgsc.2022.100283
Rubio-Martin del Campo, K. N., Rivas-Gastelum, M. F., Garcia-Amezquita, L. E., Sepulveda-Villegas, M., López-Mena, E. R., Mejía-Méndez, J. L., and Sánchez-López, A. L. (2025). "From nature to science: A review of the applications of pectin-based hydrogels," *Macromol* 5(4), article 58. https://doi.org/10.3390/macromol5040058
Said, N. S., Olawuyi, I. F., and Lee, W. Y. (2023). "Pectin hydrogels: Gel-forming behaviors, mechanisms, and food applications," *Gels* 2023, article 9090732. https://doi.org/10.3390/gels9090732
Saxena, A. K., Kumar, M., Chakdar, H., Anuroopa, N., and Bagyaraj, D. J. (2020). "*Bacillus* species in soil as a natural resource for plant health and nutrition," *Journal of Applied Microbiology* 128(6), 1583-1594. https://doi.org/10.1111/jam.14506
Sharma, B., Larroche, C., and Dussap, C.-G. (2020). "Comprehensive assessment of 2G bioethanol production," *Bioresource Technology* 313, article 123630. https://doi.org/10.1016/j.biortech.2020.123630
Shu, X., Xiong, S., Wang, Q., Yang, M., and Zhang, Q. (2025). "Chitosan-modified biochar for improving water retention in karst quarries: A potential solution for soil remediation," *Sustainability* 17(11), article 4815. https://doi.org/10.3390/su17114815
Soliman, E., and Mansour, M. M. (2024). "Enhancing soil organic carbon content and water retention using polyvinyl alcohol cross-linked with chitosan and pectin," *Journal of Soil Science and Plant Nutrition* 24(1), 791-803. https://doi.org/10.1007/s42729-023-01584-x
Staffas, L., Gustavsson, M., and McCormick, K. (2013). "Strategies and policies for the bioeconomy and bio-based economy: an analysis of official national approaches," *Sustainability* 5(6), 2751-2769. https://doi.org/10.3390/su5062751

Song, R., Qi, C., Fei, Y., Wang, B., Zhou, W., and Gao, H. (2025). "Phosphoric acid-activated shrimp shell biochar-chitosan for mitigating soil sodicity and tebuconazole contamination," *Journal of Polymers and the Environment* 33(11), 4777-4794. https://doi.org/10.1007/s10924-025-03681-7

Sultana, N. (2023). "Biological properties and biomedical applications of pectin and pectin-based composites: A review," *Molecules* 28(24), article 7974. https://doi.org/10.3390/molecules28247974

Sun, Q., Huang, M., Zeng, J., Ma, M., Li, J., and Le, T. (2025). "Beyond waste to bioactive potential: Advances in olive by-product valorization and resource recovery," *Food Chemistry* 2025, article 146727. https://doi.org/10.1016/j.foodchem.2025.146727

Ubando, A. T., Felix, C. B., and Chen, W.-H. (2020). "Biorefineries in circular bioeconomy: A comprehensive review," *Bioresource Technology* 299, article 122585. https://doi.org/10.1016/j.biortech.2019.122585

Vicente, J., Kist, V., Mega, C. P., Rossato, O. B., de Oliveira Veloso, G., and de Carvalho, M. G. (2026). "Spectroscopy-driven authentication of agro-industrial products: A comprehensive review of NMR, FT-IR, NIR and chemometric workflows," *Food Chemistry* 513, article 148982. https://doi.org/10.1016/j.foodchem.2026.148982

Walkenström, P., Kidman, S., Hermansson, A.-M., Rasmussen, P. B., and Hoegh, L. (2003). "Microstructure and rheological behaviour of alginate/pectin mixed gels," *Food Hydrocolloids* 17(5), 593-603. https://doi.org/10.1016/S0268-005X(02)00119-4

Wang, R., Li, Y., Shuai, X., Liang, R., Chen, J., and Liu, C. (2021). "Pectin/activated carbon-based porous microsphere for pb2+ adsorption: Characterization and adsorption behaviour," *Polymers* 13(15), article 2453. https://doi.org/10.3390/polym13152453

Wijitkosum, S., and Sriburi, T. (2025). "Effects of hardwood biomass variability on biochar properties: insights from wood waste utilization," *Journal of Human Earth Future* 6, 12-26. https://doi.org/10. 28991/HEF-2025-06-01-02

Zhao, J., Jiang, Y., Chen, X., Wang, C., and Nan, H. (2025). "Unlocking the potential of element-doped biochar: from tailored synthesis to multifunctional applications in environment and energy," *Biochar* 7(1), article 77. https://doi.org/10.1007/s42773-025-00467-x

Article submitted: June 3, 2026; Peer review completed: August 15, 2026; Revised version received: September 3, 2026; Accepted: September 4, 2026; Published: September 22, 2026.
DOI: 10.15376/biores.21.4.10921-10957